TECHNISCHE UNIVERSITÄT MÜNCHEN

Lehrstuhl für Biotechnologie der Nutztiere

Early Detection and Treatment Evaluation of Gastric Cancer

Wajana Lako Labisso

Vollständiger Abdruck der von der Fakultät Wissenschaftszentrum Weihenstephan für Ernährung, Landnutzung und Umwelt der Technischen Universität München zur Erlangung des akademischen Grades eines

Doktors der Naturwissenschaften

genehmigten Dissertation.

Vorsitzender:		Univ.-Prof. Dr. M. Schemann
Prüfer der Dissertation:	1.	Univ.-Prof. A. Schnieke, Ph.D.
	2.	Priv.-Doz. Dr. D. K. M. Saur

Die Dissertation wurde am 15.12.2011 bei der Technischen Universität München eingereicht und durch die Fakultät Wissenschaftszentrum Weihenstephan für Ernährung, Landnutzung und Umwelt am 09.03.2012 angenommen.

Table of contents

Table of contents I

List of tables IV

List of figures V

Abbreviations and acronyms VI

Zusammenfassung IX

Summary XI

1. Introduction 1

1.1. Gastric carcinogenesis 1

1.1.1. Incidence of gastric cancer 1

1.1.2. Classification of gastric cancer 1

1.1.3. Role of genetic and epigenetic alterations in gastric cancer 3

1.1.4. Risk factors for gastric cancer development 6

1.1.4.1. *Helicobacter pylori* infection 6

1.1.4.2. Other risk factors for gastric cancer development 6

1.2. The Semian virus 40 (SV40) T large antigen-transgenic mice 7

1.3. Early detection of gastric cancer 7

1.4. Gastric cancer treatment 8

1.5. Histone deacetylases (HDACs) and histone deacetylase inhibitors (HDACis) in cancer therapeutics 9

1.5.1. Histone deacetylases (HDACs) 9

1.5.2. Histone deacetylase inhibitors (HDACis) 11

1.6. The c-MYC transcription factor and its therapeutic implication in cancer 12

1.7. Aims of the study 14

2. Materials 15

2.1. Technical equipments 15

2.2. Disposables 17

2.3. Chemicals, reagents and enzymes 18

2.4. Kits 21

2.5. Antibodies 22

2.6. Primers 23

2.7. siRNAs 25

2.8. Inhibitors 26
2.9. Bacterial strains 26
2.10. Buffers and solutions 26
2.11. Histochemistry reagents 28
2.12. Cell Culture 29
2.13. Cell culture, reagents and media 29

3. Methods 31
3.1. Animal Experiments 31
3.2. Histological analysis and stainings 31
3.2.1. Paraffin sections 31
3.2.2. Haematoxylin and eosin (HE) staining 31
3.2.3. Immunohistochemistry 32
3.3. Cell Culture conditions and preservation of cells 32
3.4. Molecular techniques 33
3.4.1. Transformation of competent bacteria and isolation of plasmid DNA 33
3.4.2. Screening potential biomarker genes for imaging gastric cancer 33
3.4.3. RNA isolation and quantitative PCR (qPCR) 34
3.4.4. Protein isolation and detection 34
3.4.5. Western blot 35
3.4.6. siRNA transfection 35
3.4.7. Quantitative chromatin immunoprecipitation (qChIP) 36
3.4.8. Annexin V staining 36
3.5. Treatment of cells with various inhibitors and viability assay 37
3.5.1. Treatment of cells with various inhibitors 37
3.5.2. Viability assay 37
3.5.3. Hoechst staining 38
3.6. Statistical analysis 38

4. Results 39
4.1. Early detection of gastric cancer 39
4.1.1. Identification of cathepsins and MMPs as potential tools for molecular imaging in gastric cancer 39
4.1.2. Activation of the cathepsin-activable NIRF probe in gastric cancer 42
4.2. Treatment evaluation of gastric cancer 44

4.2.1. Response of gastric cancer cell lines to HDACis 44
4.2.2. BCL_{XL} and MCL1 expression levels inversely correlate with the responsiveness of gastric cancer cells towards HDACi 47
4.2.3. BCL_{XL} and MCL1 counteract efficacy of HDACi 48
4.2.4. c-MYC controls BCL_{XL}, MCL1 and the HDACi response 49
4.2.5. c-MYC-induced transcription of *eIF4E* regulates BCL_{XL} expression in gastric cancer cells 53

5. Discussion 57
5.1. Early detection of gastric cancer 57
5.2. Treatment evaluation of gastric cancer 59

6. Conclusions 62

7. Bibliography 63

8. Curriculum Vitae ..... Error! Bookmark not defined.

9. Acknowledgements 77

List of tables

Table 2-1: Technical equipments used in this study. 15
Table 2-2: Disposables used in this study. 17
Table 2-3: Chemicals, reagents and enzymes used in this study. 18
Table 2-4: Kits used in this study. 21
Table 2-5: Antibodies used in this study. 22
Table 2-6: Human primer sets applied in qPCR. 23
Table 2-7: Murine primer sets applied in qPCR. 25
Table 2-8: siRNAs used in this study. 25
Table 2-9: Inhibitors used in this study. 26
Table 2-10: Bacterial strains used in this study. 26
Table 2-11: Buffers and solutions used in this study. 26
Table 2-12: Histochemistry reagents used in this study. 28
Table 2-13: Cell lines used in this study. 29
Table 2-14: Used reagents for cell culture. 29
Table 3-1: Dilutions of primary antibody for Western blot. 37
Table 3-2: Working concentrations of inhibitors used in this study. 38
Table 4-1: Response of gastric cancer cell lines against SAHA treatment. 44
Table 4-2: Response of gastric cells lines to 4SC-201 and 4SC-202. 46

List of figures

Figure 1-1: Anatomical sites of gastric cancer. 2
Figure 1-2: Histological types of gastric cancer. 3
Figure 1-3: The main genetic and epigenetic alterations in gastric carcinogenesis. ... 4
Figure 1-4: Major classes of HDACs with their functional/structural domains and inhibitors.. 11
Figure 1-5: Functional domains of human c-MYC protein..... 13
Figure 4-1: mRNA expression of cathepsin (Cts) and matrix metalloproteinases (MMPs) in human gastric cancer cell lines. 39
Figure 4-2: mRNA expression of cathepsin (Cts) and matrix metalloproteinases (MMPs) in murine gastric cancer cell lines and tissues. 40
Figure 4-3: Immunohistochemistry of cathepsins (Cts) and matrix metalloprotinses (MMPs) in murine stomach. 41
Figure 4-4: Cathepsins activate NIRF-activable probe. 43
Figure 4-5: Dose dependent response of gastric cancer cells to SAHA treatment ... 44
Figure 4-6: SAHA induces apoptosis in gastric cancer cell lines. 45
Figure 4-7: Dose dependent response of gastric cancer cell lines to 4SC-201 and 4SC-202 treatment. 46
Figure 4-8: BCL_{XL} restricts SAHA efficacy of gastric cancer cells..... 47
Figure 4-9: MCL1 restricts SAHA efficacy of gastric cancer cells. 49
Figure 4-10: c-MYC controls MCL1 and BCL_{XL} expression of gastric cancer cells... 50
Figure 4-11: c-MYC knockdown reduces viability of gastric cancer cell lines. 51
Figure 4-12: c-MYC induces apoptosis in gastric cancer cells..... 52
Figure 4-13: *MCL1* is a direct c-MYC target in gastric cancer cells. 53
Figure 4-14: c-MYC controls *eIF4E* transcription to regulate BCL_{XL} expression in gastric cancer cells. 55

Abbreviations and acronyms

Abbreviations and acronyms	Descriptions
AFN	Atipamezole flumazenil naloxone
APC	Adenomatous polyposis coli
ATP	Adenosine triphosphate
BCL_{xL}	B Cell Lymphoma 2-like 1
bp	Base pairs
BSA	Bovine serum albumin
CagAPI	CagA pathogenecity island
CCD	Charge coupled device
CDK	Cyclin-dependent kinase
cDNA	Complementary desoxyribonucleic acid
CEA	Carcinoembryonic antigen A
cm	Centimeter
CO_2	Carbondioxide
c-MYC	Cellular myelocytomatosis
CTCL	Cutaneous T-cell lymphoma
dCTP	2'-deoxycytidine 5'-triphosphate
DMEM	Dulbecco’s Modified Eagle Medium
DMSO	Dimethylsulfoxide
DNA	Desoxyribonucleic acid
EDTA	Ethylenediaminetetraacetic acid
EGF	Epithelial growth factor
EGFP	Enhanced green fluorescent protein
eIF4E	Eukaryotic translation initation factor 4E
et al	et alii
EtBr	Ethidiumbromide

EtOH	Ethanol
FCS	Fetal calf serum
FDA	food and drug authority
g	G force
g	Gram
HDAC	Histone deacetylase
HDACi	Histone deacetylase inhibitors
HDGC	Hereditary diffuse gastric cancer
h	Hour
H_2O	Water
HE	Haematoxylin eosin
HLHLZ	Helix–loop–helix leucine zipper
IARC	International agency for research in cancer
i.p.	Intraperitoneal
i.v.	Intravenous
kb	Kilo base
kg	Kilogram
MCL1	Myeloid cell leukemia sequence 1
MTT	3-(4,5-dimethylthiazol-2-yl)-2,5-diphenyltetrazoliumbromide
NF-κB	Nuclear factor kappa-light-chain-enhancer of activated B cells
ng	Nano gram
nm	Nano meter
Nmol	Nano molar
OD	Optical densitiy
P	Phospho
PanIN	Pancreatic intraepithelial neoplasia
PBS	Phosphate buffered saline
PCR	Polymerase chain reaction
PDAC	Pancreatic ductal adenocarcinoma

RNA	Ribonucleic acid
rpm	Rounds per minute
RT	Room temperature
SID	Sin3-interaction domain
SAHA	Suberoylanilide hydroxamic acid
SDS	Sodium dodecyl sulfate
sec	Second
SV40	Semian virus 40
Tag	T large antigen
TGFβ	Transforming growth factor β
U	Units
UGIT	Upper gastrointestinal tract
UV	Ultra violet
V	Volt
v-MYC	Viral myelocytomatosis
WHO	World Health Organization
WT	Wild type
µg	Microgram
µl	Microliter

Zusammenfassung

Die Prognose des Magenkarzinoms ist mit einer 5-Jahresüberlebensrate von weniger als 20% weiterhin sehr schlecht. Daher ist es dringed erforderlich neue Strategien zur Früherkennung von präkanzerösen und malignen Läsionen zu entwickeln sowie neue Therapiestrategien zu etablieren. In dieser Arbeit wurden im murinen *CEA-TAG* Magenkarzinommodell sowie in drei humanen und zwei murinen Magenkarzinom-zelllinien die Cathepsine B und H sowie die Matrixmetalloprotease (MMP) MMP2 identifiziert, die „nah-infrarot“ (NIRF) Sonden aktivieren können. Die entsprechenden Proteasen zeigen eine hohe Expression sowohl in den Zelllinien als auch in den untersuchten murinen Magenkarzinomen auf mRNA und Proteinebene im Vergleich zu normaler Magenantrummukosa. Mit Hilfe der proteaseaktivierbaren NIRF-Sonde konnten Magenkarzinome *in vivo* markiert und mit Hilfe eines NIRF-Scanners *ex vivo* detektiert werden. Daher könnten Cathepsin B, H und MMP2 aktivierbare NIRF Sonden zur endoskopischen Früherkennung des Magenkarzinoms in Zukunft eingesetzt werden. Desweiteren wurde in dieser Arbeit die Wirkung von Histondeacetylase Inhibitoren (HDACi) auf Magenkarzinomzellen untersucht. Dazu wurden sechs humane und zwei murine Zelllinien mit drei unterschiedlichen Inhibitoren behandelt. Mittels MTT und Fluorometrie wurden Viabilität und Apoptose der Zelllinien ermittelt. Dabei wurden unterschiedliche Sensitivitäten der verwendeten Zelllinien gegenüber HDAC Inhibitoren beobachtet. Zur Analyse der molekularen Resistenzmechnismen dieser Zelllinien wurden Westernblotanalysen, qPCR, RNAi und qChIP Experimente durchgeführt. Dabei wurde eine erhöhte Expression der antiapoptotischen BCL2 Familienproteine BCL_{XL} und MCL1 in HDAC Inhibitor insensitiven Zellen festgestellt werden. RNAi vermittelte Inhibition von BCL_{XL} und MCL1 zeigte dabei eine erhöhte Sensitivität der Zellen gegenüber SAHA. Um potentielle Signalwege zu finden die BCL_{XL} und MCL1 regulieren, wurden verschiedenen Transkriptionsfaktoren untersucht. Dabei konnte c-MYC als Hauptregulator beider antiapoptotischen Proteine identifiziert werden. Pharmakologische Hemmung oder RNAi vermittelte Depletion von c-MYC erhöhte dementsprechend die SAHA Sensitivität. Es konnte weiter gezeigt werden, dass c-MYC *MCL1* transkriptionell direkt aktiviert, wohingegen BCL_{XL} indirekt durch *eIF4E* reguliert wird. Dabei aktiviert c-MYC den Translationsinitiationsfaktor eIF4E der die direkte Translation von BCL_{XL} steuert. Die Inhibition von c-MYC in Kombination mit

HDAC Inhibitoren könnte daher eine vielversprechende Option für künftige Therapiestrategien beim Magenkarzinom sein.

Summary

To improve the prognosis of gastric cancer patients, novel strategies for early detection of precancerous and cancerous lesions, tumor stage-adapted therapy and monitoring of therapeutic response are urgently needed. In this study, we used the murine *CEA-TAG* gastric cancer model and 3 human and 2 murine gastric cancer cell lines to identify cathepsins and matrix metalloprotinases (MMPs) proteases as near-infrared fluorescent (NIRF) probe activators in gastric cancer. The results show high protein and mRNA expression levels of cathepsins B, H and MMP2 in the human and murine gastric cancer cell lines. In addition, expression of the proteases was markedly increased in murine primary gastric cancer speciesmens compared to normal gastric mucosa. Accordingly, the NIRF probe was specifically activated in stomach tumor of *CEA-TAG* mice and allowed *ex vivo* detection of the tumor by Odyssey planar near-infrared scanner. These results indicate that cathepsins B, H and MMP2 are promising biomarkers for early endoscopic detection of gastric cancer. To evaluate the efficiency of HDACi for gastric cancer treatment a panel of human and murine gastric cancer cell lines were investigated. The result indicated that MKN45 (SAHA IC50=3.2, 95% CI= 2.6-3.9) and ST2957 (IC50=2.8, 95% CI=2.1-3.7) cell lines were among the top non-responding cells to SAHA treatment whereas MGC8 (IC50=1.0, 95% CI=0.7-1.3 95%) was observed to be relatively the most sensitive. First, it was observed that BCL_{XL} and MCL1 expression levels inversely correlated with the responsiveness of gastric cancer cells towards SAHA. The efficacy of SAHA was augmented by siRNAs directed against BCL_{XL} and MCL1 in nonresponding cell lines. Subsequently, potential pathways were tested if they were involved in regulating BCL_{XL} and MCL1 expression in these cell lines. Two independent mechanisms, by which c-MYC protects gastric cancer cells from HDACi, were identified. Firstly, c-MYC directly regulates transcription of *MCL1* and secondly, regulation of BCL_{XL} protein expression was due to c-MYC`s ability to control the *eIF4E* gene and thereby translation of the *BCL_{XL}* mRNA. Our observation that c-MYC controls expression of important anti-apoptotic BCL2 family members might argue that c-MYC is an important mediator of therapeutic resistance of gastric cancer cells. Since MCL1 and BCL_{XL} are regulated by c-MYC in gastric cancer cells, c-MYC inhibition applied in combination with HDACi might be a rationally based therapeutic option for this type of cancer.

1. Introduction

1.1. Gastric carcinogenesis

Gastric cancers include malignancies that arise in any part of the stomach. Accordingly, several different types of cancer can take place in the stomach; however adenocarcinomas account for majority of gastric malignancies (Smith, 2006). Over 90% of gastric adenocarcinomas are attributed to chronic *Helicobacter pylori* (*H.pylori)* infection and mostly affects the antral parts of the stomach (Fox and Wang, 2007). The remaining small proportion of the stomach carcinogenesis is due to lymphomas that originate in the B and T cells of the lamina propria and sarcomas, which arise from the cells of the muscle layer. Furthermore, carcinoid tumours are also believed to arise from neuroendocrine cells (Shang and Pena, 2005; Smith *et al.,* 2006).

1.1.1. Incidence of gastric cancer

Despite huge investments and tremendous investigations in the field of cancer, gastric cancer remains one of the most deadly diseases worldwide. It is the second cancer-related killing disease, only next to lung cancer, and the 4th frequent type of cancer (Hu *et al*., 2007). Gastric adenocarcinoma accounts for over 1 million cases and 10.4% of global annual cancer mortality, two-thirds of which occurs in developing countries (Lochhead and El-Omar, 2008; Parkin *et al*., 1999). Due to delayed diagnosis and the lack of efficient treatment options for advanced tumors, gastric cancer is characterized with extremely poor prognosis with a 5 year survival rate of less than 20% (Jemal *et al*., 2007). This is attributed mainly to late detection and absence of efficient treatment options for advanced tumors. Regarding the distribution of global gastric adenocarcinoma, Asia (particularly, Japan, Korea and china), Eastern Europe and the Andean region of South America, with diverse geographical characteristics are more seriously affected than other parts of the world human populations (Hu *et al*., 2007).

1.1.2. Classification of gastric cancer

Anatomically, gastric adenocarcinoma can be classified as proximal (cardiac cancer) and distal (non-cardiac) gastric adenocarcinomas, the former being located within 2 cm of the esophagogastric junction and reported not to be associated with

Helicobacter pylori infection (*H. pylori* hereafter). On the other hand, the distal (also termed as non-cardia cancer) is strongly linked to *H. pylori* infection and located in the antrum region of the stomach (Figure 1-1). According to the histopathological courses of changes during gastric cancer progression and architecture of the grandular structures, gastric adenocarcinomas can be classified into well differentiated intestinal type tumors and undifferentiated diffuse type tumors that have different histological, epidemiological and prognostic features (Carneiro *et al*., 2008; Catalano *et al*., 2005). Advances in genetic studies and histopathologies indicated that the development of intestinal type gastric cancer is a multi-step process (Figure 1-2) characterized by intestinal metaplasia through dysplasia and adenocarcinoma (Johnson and Evers, 2008).

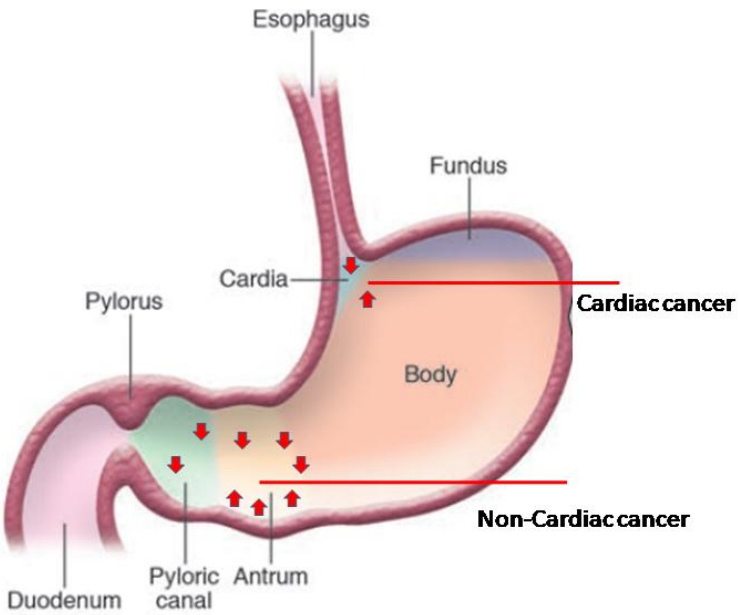

Figure 1-1: Anatomical sites of gastric cancer. (Modified from Fox and Wang, 2007)

Moreover, intestinal type tumors are characterized by a corpus-dominated gastritis with gastric atrophy and intestinal metaplasia. They usually take place in late aged men than females whereas diffuse type gastric cancers commonly affect younger men and women equally and composed of individually infiltrating neoplastic cells that do not form glandular structures (Lochhead and El-Omar, 2008). Intestinal tumours are usually well differentiated and distinguished by structures similar to functional glands of the gastrointestinal tract (Figure 1-2a) whereas the diffuse-type adenocarcinomas display reduced cell cohesion and tend to substitute the gastric mucosa by signet-ring cells (Figure 1-2b). The course of evolution for both tumors is

exclusively different and both are featured by distinct molecular changes (Figure 1-3). For example, one common steps in intestinal types of gastric cancer is gastritis, which progresses to mucosal atrophy (atrophic gastritis) followed by intestinal metaplasia, dysplasia and adenocarcinoma. This progression to adenocarcinoma in the route of succession of histolgical transformations from precancerous lesions through intestinal metaplasia and dysplasia is known as the Correa pathway (Correa *et al.,* 1975) (Figure 1-2a). No preceding steps have been observed in the pathogenesis of diffuse tumours (Figure 1-2b)

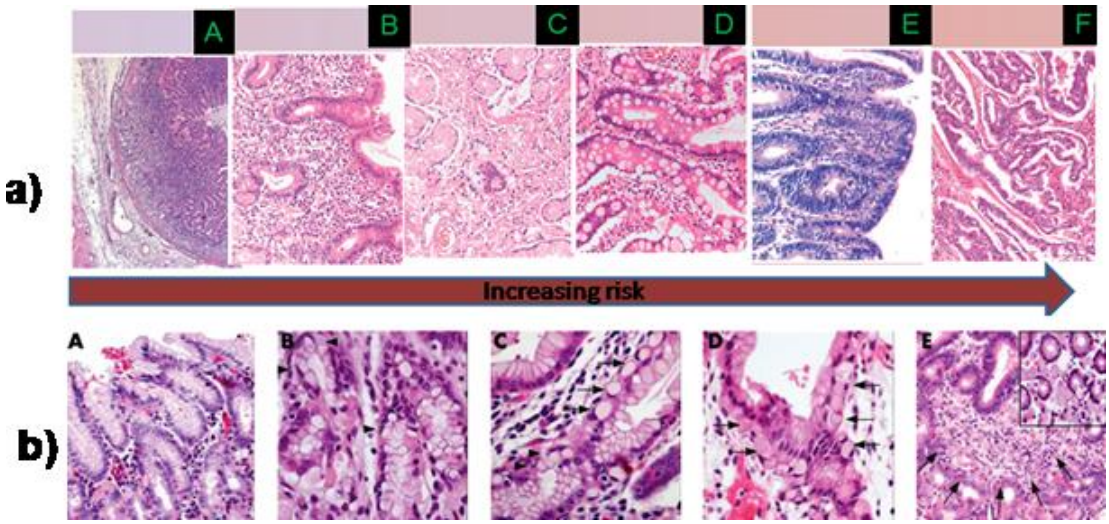

Figure 1-2: Histological types of gastric cancer. a) Indicates Correa pathway **(A)** Normal mucosa. **(B)** Chronic gastritis. **(C)** Mucosal atrophy. **(D)** Intestinal metaplasia. **(E)** Dysplasia. **(F)** Intestinal-type carcinoma (Hartgrink *et al*., 2009)**.**
b) Histological alterations in diffuse gastric cancer **(A)** Mild chronic gastritis and foveolar hyperplasia. **(B)** Glands with intact basement membrane lined by signet ring cells. **(C-D)** Spread of signet ring cells below the preserved epithelium of glands. **(E)** Early invasive intramucosal signet ring cell carcinoma (Carneiro *et al*., 2008).

1.1.3. Role of genetic and epigenetic alterations in gastric cancer

Several genetic and epigenetic aberrations in oncogenes, tumour suppressor genes, cell-cycle regulators, cell adhesion molecules, DNA repair genes and microsatellite instability as well as telomerase activation are observed in intestinal type gastric adenocarcinomas (Figure 1-3). Loss of expression of the tumour suppressor genes *p53, p73, TFF1* and *APC* (Adenomatous polyposis coli) is frequently described in intestinal-type gastric adenocarcinomas (Nakatsuru *et al*., 1992; Smith *et al*., 2006).

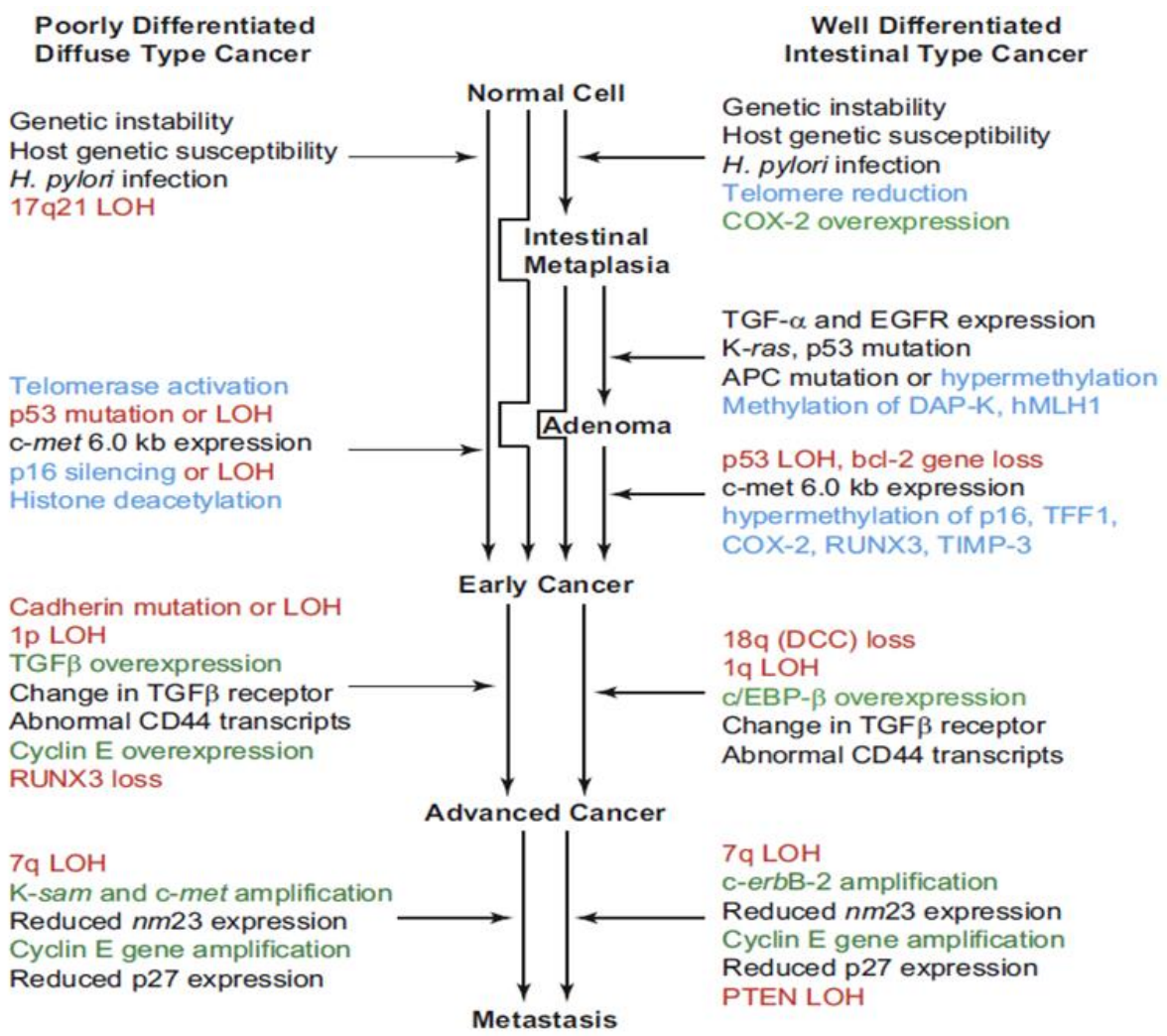

Figure 1-3: The main genetic and epigenetic alterations in gastric carcinogenesis. (Johnson and Evers, 2008).

Silencing of a gastric specific trefoil factor *(TFF1*) resulted in development of dysplasia, adenoma and gastric carcinoma in mice (Lefebvre *et al*., 1996). Loss or reduction of tumor suppressor gene *TFF1* due to DNA methylation in its promoter region have been observed in intestinal metaplasia and gastric adenomas, indicating a key role of *TFF1* in progression of intestinal-type adenocarcinoma (Clyne *et al*., 2004; Tahara, 2004). Missense mutations in *APC* gene are also frequently detected in intestinal-type tumours and the silencing of *APC* enhances the activation of the downstream target gene of APC-β-catenin pathway, which inturn serves as an oncogene (Nakatsuru *et al*., 1992). Similarly, alteration of some other genes like *RUNX3* and *FHIT* are also frequently detected in intestinal adenocarcinomas. Proto-oncogene *c-erbB2* is also highly amplified in intestinal-type cancers and its overexpression has been interestingly related to poorer prognosis (Gravalos and Jimeno, 2008). Likewise, amplification or overexpression of the cell cycle regulator

cyclin E, has been associated with aggressiveness and lymph node metastasis (Akama *et al*., 1995). Epigenetic silencing of the mismatch repair gene *hMLH1*, *p27* gene downregulation, transcriptional alteration of *CD44*, microsatellite instability of the *D1S191* locus, deregulations of miRNAs and overexpression of the growth factors of the EGF family such as EGF, TGF-α, IGF II and bFGF are reported to be hallmarks of intestinal-type tumors (Guo *et al*., 2011).

The underlying molecular mechanisms involved in diffuse-type gastric adenocaricnoma include aberration of oncogenes, tumour suppressor genes and cell cycle regulators, as well as genetic instability and modifications in growth factors and cytokines (Figure 1-3). Overexpressions of a number of proto-oncogenes are frequently observed in diffuse-type gastric carcinoma. For example, the tyrosine kinase receptor gene *c-Met*, encoding for hepatocyte growth factor receptor, is amplified in 39% of diffuse-type gastric tumours (Kuniyasu *et al*., 1992). Overactiavation of the Type II *Ksam* oncogene, which encodes a receptor for keratinocyte growth factor, is frequently detected in gastric cancer. *Ksam* is preferentially amplified in more than one-third of advanced diffuse-type gastric tumours. Moreover, overactivation of this gene is associated with poorer prognosis (Hattori *et al*., 1990).

More importantly, the E-cadherin tumour suppressor gene (*CDH1*) plays an important role in the carcinogenesis of the diffuse-type gastric adenocarcinomas. More than 50% of somatic mutations in the *CDH1* gene have been reported only in sporadic diffuse type gastric cancer, but not in intestinal-type gastric cancer (Lynch *et al*., 2005). Interestingly, in mixed gastric carcinomas loss of E-cadherin expression has been limited only to the diffuse parts of the tumour, indicating that E-cadherin loss might be the underlying genetic hallmark for the difference between diffuse and intestinal gastric adenocarcinomas (Machado *et al*., 1999; Johnson and Evers, 2008)

Most of gastric adenocarcinomas occur sporadically, however few cases of gastric cancers take place in a noticeably inherited predisposition syndromes. One of these syndromes is the hereditary diffuse gastric carcinoma (HDGC) that is an autosomal dominantly inherited gastric cancer susceptibility syndrome caused by germline mutations in the *CDH1* gene (Guilford *et al*., 1998).

Another tumour suppressor gene altered in diffuse-type gastric adenocarcinomas is the *TP53* gene that is frequently silenced in gastric carcinoma by loss of heterozygosity (LOH), missense mutations and frame-shift deletions, being GC-AT transitions common in diffuse-type carcinomas (Yokozaki *et al*.,1992).

1.1.4. Risk factors for gastric cancer development

1.1.4.1. *Helicobacter pylori* infection

Inspite of the fact that myriads of scientific efforts and investments have been put on bacterial eradication, *H.pylori* infect more than 70 and 40% of the human population in developing and developed countries, respectively (Correa and Houghton, 2007; Hartgrink *et al*., 2009; Smith *et al*., 2006). Still, infection with *H. pylori* remains to be responsible for inducing chronic gastric inflammation that progresses to atrophy, intestinal metaplasia, dysplasia and gastric adenocarcinoma. Therefore, the international agency for research in cancer (IARC) catagorized the infection with *H.pylori* as a Class I human carcinogen (Peek and Blaser, 2002; Rugge *et al*., 2003). Over 90% of intestinal type of adenocarcinoma is linked to infection with these bacteria, which are Gram-negative, spiral shaped, microaerophilic bacilli that colonize the gastric epithelium and represent the most common bacterial infection worldwide (Smith *et al*., 2006). All *H. pylori* strains cause chronic gastric mucosal inflammation, but a few bacteria that are endowed only with Cag A pathogenecity islands (CagApI) are linked with high risk of gastric adenocarcinomas development. *H. pylori* induced gastric inflammation is characterized by the presence of infiltrating macrophages, B and T lymphocytes, polymorphonuclear cells and plasma cells (Zambon *et al*., 2005). Gastritis is the beginning stomach disorder that promotes *H. pylori*-induced damage, and its progression and spreading out determine the clinical outcome of the patient.

1.1.4.2. Other risk factors for gastric cancer development

Besides strong evidences implicating *H. pylori* as the main etiological factor for gastric cancer development, several other environmental risk factors are also indicated to promote gastric cancer development (Compare *et al*., 2010; Shikata *et al*, 2006). Of note are chronic gastric inflammations, eating highly salted (Joossens *et al*., 1996; Peleteiro *et al*., 2011) and smoked foods (Kono and Hirohata, 1996) and low intake of foods rich in anti-oxidants such as fruits and vegetables (Tsugane and Sasazuki, 2007; WHO, 2003). Eating foods that have not been prepared or stored

properly, being older or male, smoking cigarettes, alcoholism, and family history with gastric cancer are also potential risk factors for gastric cancer development (Compare *et al*., 2010; Joosens *et al*., 1996; Peleteiro *et al.*, 2011).

1.2. The Semian virus 40 (SV40) T large antigen-transgenic mice

Genetically engineered mice are essential tools for preclinical study of human cancers, including gastric cancer. One of the most recent and robust mouse models for human gastric cancer study is a semian virus 40 large T antigen (SV40 Tag) transgenic mice (Thompson *et al*., 2000). In this model, the *SV40 Tag* is regulated by a human carcinoembryonic antigen (*CEA*) gene promoter. The *CEA* is commonly used as a marker for a number of cancer types and expressed in several types of human cancers, including more than half of gastric cancer (Nöckel *et al*., 2006). The SV40 Tag is a powerful antigen that has been used to produce tumors under the control of tissue specific gene promoter in transgenic mice. It is a viral oncoprotein that promots the early oncogenic transformation of cells by modulating several cellular activities in genome integrity and cell cycle. Thus, cellular transformation by *SV40 Tag* is mediated by the functional deregulation of key cell cycle regulators such as pRB, p53 and p300 protein family members (Ali and DeCaprio, 2001). The SV40 *Tag* transgenic gastric cancer mouse model is reported as so efficient mouse model that it displays dysplastic crypts in the antrum-region at the age of a month. Dysplasia of these mice immediately progresses to aggressive forms of pyloric adenocarcinoma within the age of 2 months. Finally, *SV40 Tag* transgenic mice were overwhelmed by the overload and blokage of pylori by tumor at the age of 3 to 4 months. This results in extreme weight lose and finally the end of the life of the mouse (Nöckel *et al*., 2006; Thompson *et al*., 2000). Thus, the timely course of dysplastic crypts formation, the progression of dysplasia into invasive carcinoma, gradual increase in tumor load and the short time required to develop tumor may enable these mice an ideal preclinical models for detecting and monitoring gastric cancer (Hance *et al*., 2005).

1.3. Early detection of gastric cancer

A critical step to improve the outcome of gastric cancer patients is to detect early gastric cancer and gastric lesions at their premalignant stages, thereby permitting

minimal invasive therapy. Thus far, high grade dysplasia and early gastric cancers are often missed during conventional endoscopic examination of the upper gastrointestinal tract (UGIT) (Enns, 2010; de Vries *et al.,* 2007 ; Leodolter *et al*., 2006). Despite the application of novel endoscopic imaging techniques like chemoendoscopy and magnification endoscopy, a substantial high miss rate of 19% has been reported for early gastric cancer in Japan (Lambert, 2002). Therefore, the development of highly sensitive and specific techniques for preneoplastic lesions and early gastric cancer detection is urgently needed.

The visualization of specific biomarkers for precursor lesions and early gastric cancer represents probably a crucial tool to improve the accuracy of upper gastrointestinal endoscopy. Recent progress in imaging research indicated that molecular imaging in animal models is possible using antibodies or ligands, labeled with radioactives or flourophores (Eser *et al*., 2011; Mahmood and Weissleder, 2003; Weissleder, 2006; Weissleder and Mahmood, 2001). In addition, activable near infrared fluorescence (NIRF) imaging probes (“smart probes”) for preneoplastic and neoplastic lesions have been shown to detect adenomas in the $APC^{min/+}$ mouse models. These “smart probes” are specifically activated by tumor specific proteases. Even lesions smaller than 500µm that were macroscopically invisible were detected with the aid of smart probes, indicating that these probes can be used for early detection of adenomas (Weissleder, 2006). However, no data are available for imaging of precursor lesions and early gastric cancer in animal models and humans. Likewise, no biomarkers are reported in this regard as indicators to detect precursor lesions and early gastric cancers.

1.4. Gastric cancer treatment

Despite the record of marked decline in gastric cancer incidence and mortality over the last decades in most countries, gastric cancer still poses a major health problem, with nearly one million newly diagnosed cases per year (Johnson and Evers, 2008). Because of the absence of well characterized molecular biomarkers, which enable precursor lesions and early gastric cancer detection, lack of efficient therapeutic means and growing chemo-resistance of cancer cells rates (Weichert *et al.,* 2008), the effort to minimize the impact of gastric cancer remains inefficient. Likewise, poor

survival of gastric cancer patients at advanced stages is attributed to lack of efficient treatment options.

So far, complete resection at loco-regional stage of disease is the only therapeutic means with curative possibility for gastric cancer (Wacheck *et al*., 2006). Nonethless, gastric cancer is detected either at an advanced stage or relapse after apparently curative surgery. For such patients, the only available treatment option is systemic chemotherapy (Macdonald, 2003; Wacheck *et al*., 2006). Regardless of some improvements in response rates and total survival, gastric cancer at advanced stage remains an incurable disease (Weichert *et al*., 2008). Therefore, three most crucial clinical challenges are waiting to combat the devastating effects of gastric cancer in future:

1) Detection of preneoplastic lesions (low and high grad dysplasia) and early gastric cancer
2) Prevention of the progression of preneoplastic lesions and early gastric cancer into invasive adenocarcinoma
3) Defining new therapeutic strategies and establishing efficient treatment means

Despite thorough efforts to improve the outcome of cancer patients, treatment efficacy of gastric cancer patients at advanced stage of disease still remains an open question (Haglund and Wallner, 2004). Combination regimens of different chemotherapeutics often improved median survival of patients only in the range of few months (Wagner *et al*., 2005). Hence, novel therapeutic approaches are urgently needed to improve the outcome of gastric cancer patients.

1.5. Histone deacetylases (HDACs) and histone deacetylase inhibitors (HDACis) in cancer therapeutics

1.5.1. Histone deacetylases (HDACs)

The taxonomy of mammalian histone deacetylases (HDACs) is based on phylogenetic analysis, sequence homology and function of yeast HDACs. Accordingly, 18 different mammalian HDACs have been identified and are currently grouped into 4 different classes (Figure 1-4). The zinc-dependent HDACs are further sub- grouped into class I (HDAC1, 2, 3, and 8), class II (HDAC4, 5, 6, 7, 9,and 10),

and class IV (HDAC11) enzymes whereas the NAD+-dependent sirtuins (SIRT1-7) represent class III (Yang and Seto , 2008). HDAC enzymes differ in their subcellular localization, catalytic activity, and sensitivity to various inhibitors. Class I HDACs are confined to the nucleus, whereas HDAC3 has both nuclear import (NIS) and export (NES) signals being able to localize to the cytoplasm (Bolden *et al*., 2006). HDAC11 is the only member of class IV and limited to the nucleus while class II HDACs are able to shuttle in and out of the nucleus according to the signals they receive. The class III sirtuin family (SIRT1-7) has different localizations. Whereas three SIRT proteins (SIRT1, SIRT6, and SIRT7) reside in the nucleus, SIRT3, SIRT4, and SIRT5 are found in the mitochondria and SIRT2 is a cytoplasmic protein (Choi *et al*., 2001).

HDACs play several roles in normal cellular physiology and involved in the regulation of proliferation, apoptosis, differentiation, migration and angiogenesis of cancer cells (Glozak and seto, 2007; Müller and Krämer, 2010). The expressions of genes encoding for HDACs have been modulated in a number of cancer types and the deregulation of transcriptional repression facilitated by HDACs contributes to carcinogenesis of various tumors, including gastric cancer (Glozak and Seto, 2007; Münster *et al*., 2011; Mutze *et al*., 2010; Weichert, 2008). The simultaneous nuclear expression of HDAC 1, 2 and 3 has been strongly correlated with poor survival rates (Weichert *et al*., 2008) and over expression of HDAC1 has been indicated as a predictor of poor survival in 5-Fluorouracil (5-FU)/platinum-responsive gastric cancer patients (Mutze *et al*., 2010). These indicate that HDACs are promising therapeutic targets for combating cancer.

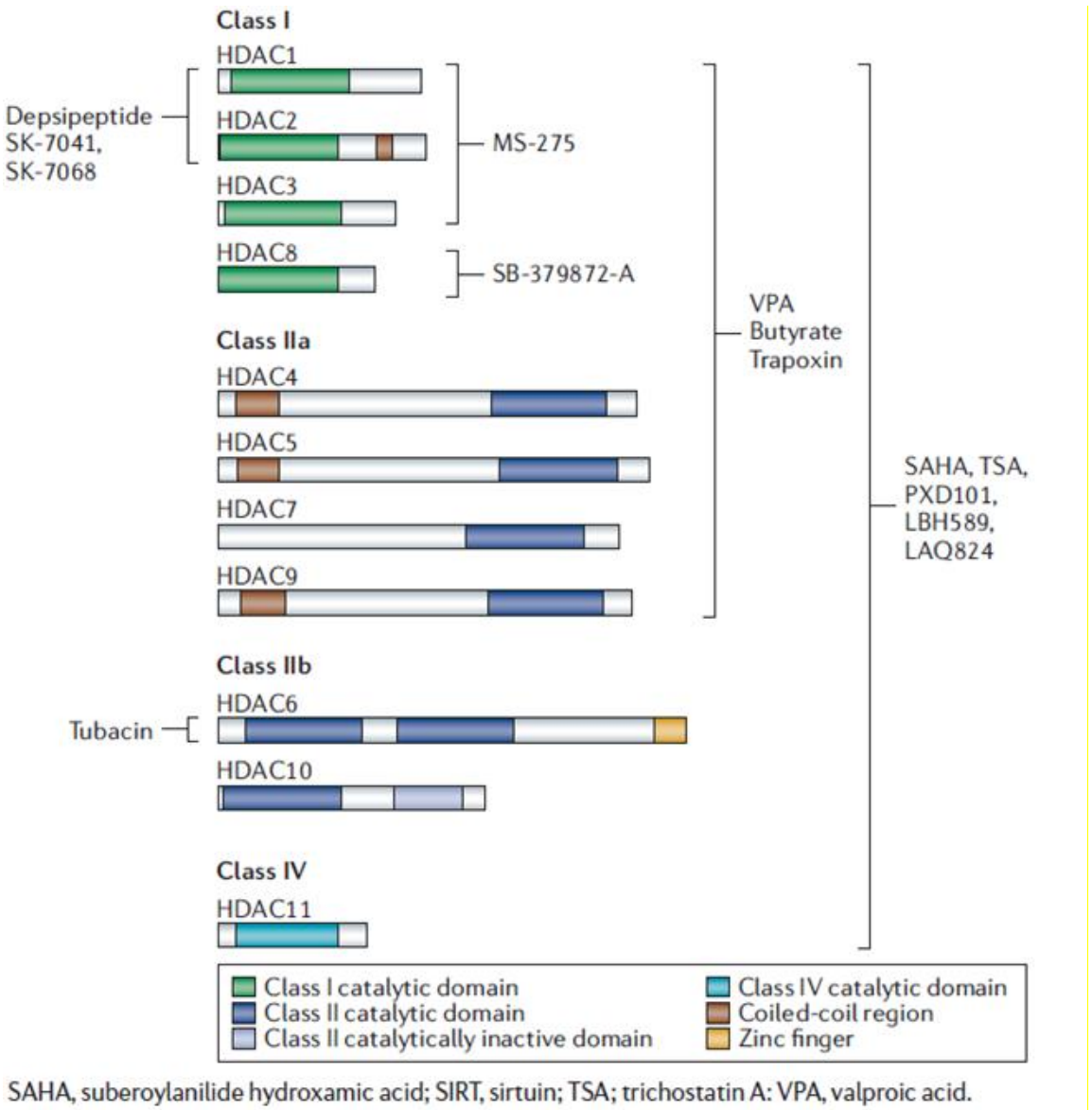

Figure 1-4: Major classes of HDACs with their functional/structural domains and inhibitors. (Bolden *et al*., 2006).

1.5.2. Histone deacetylase inhibitors (HDACis)

One of the promising emerging means in fighting cancer are the HDAC inhibitors, which are classified into at least 5 (Figure 1-4) distnict groups based on their chemical structures. These are short-chain fatty acids such as butyric acid, hydroxamic acids such as suberoylanilide hydroxamic acid (SAHA), electrophilic ketones, benzamides such as MS-275 and cyclic peptides such as depsipeptide FK-228 (Hess-Stumpp *et al*., 2007; Minucci and Pelicci, 2006; Walkinshaw and Yang, 2008). HDACis induce growth arrest, differentiation and apoptosis of cancer cells *in vitro* and *in vivo* (Gallinari *et al*., 2007; Xu *et al*., 2007). The hydroxamic-acid pan-HDACi suberoylanilide hydroxamic acid (SAHA; Vorinostat) and the cyclic peptide depsipeptide (Romidepsin; FK-228), which preferably inhibits class I HDACs, have

been approved by the USA food and drug authority (FDA) for the treatment of cutaneous T-cell lymphoma (CTCL) (Glozak and Seto, 2007).

HADCs play a very important role in carcinogenesis (Lindemann *et al*., 2007) and HADCis have been applied for the treatment of several cancer types (Frew *et al*., 2009). This is because HADCis induce growth inhibition, cell cycle arrest and apoptosis in several cancer cells. In addition, they increase the sensitivity of cancer cells to chemotherapy and ionizing radiation when synergistically applied (Lindemann *et al*., 2007). HDACis can also inhibit the angiogenesis invasion and metastasis of cancer cells (Marks *et al*., 2010). However, increasing evidence has clearly indicated that the ways how HADCis act on cancer cells are complex and vary among cancer types. Therefore, identifying their precise mechanisms of action is an area of great interest in the contemporary era of therapeutic evaluation of HDACis as anticancer agents (Walkinshaw and Yang, 2008).

1.6. The c-MYC transcription factor and its therapeutic implication in cancer

The MYC transcription factor is an important member of basic-helix–loop–helix–leucine zipper (bHLHZ) protein family that encodes the transcription factor proteins N-MYC, c-MYC, and L-MYC (Blackwood and Eisenman, 1991; Pelengaris *et al*., 2002). The MYC proetein family members play great role in regulation of several cellular functions such as cell proliferation, cell cycle progression, embryogenesis, differentiation and apoptosis. In addition to regulating several cellular physiologies, the *c-MYC* oncogene, located at chromosomal band 8q24, is involved in regulating the expression of a large number of downstream genes that carry out various cellular responses (Grandori *et al*., 2000).

The transcriptional factor c-MYC heterodimerizes with its partner protein-MAX and activates different groups of genes (Dang *et al*., 2006; Eilers and Eisenman, 2008). The carboxy-terminal basic-helix–loop–helix–lucine–zipper (bHLHLZ) domain of c-MYC binds MAX (also a bHLHLZ protein) to form MYC–MAX heterodimer that is able to bind specific c-MYC-responsive DNA sequences in the target genes. This specific DNA sequence is composed of CACGTG nucleotides and called the E-boxes (Blackwood and Eisenman, 1991; Pelengaris *et al*., 2002). The whole complex induces transcription through the association of conserved MYC-boxes I and II with the transcriptional coactivators TRAPP and BAF53 II and their corresponding histone

acetyltransferases (HATs) and ATPase/helicases (TIPs). The MYC-MAX hetero-dimerization involves also helix–loop–helix (HLH) and juxtaposed leucine zipper (Zip) domains whereas DNA binding is conferred by a basic region (Amati *et al*., 1992, Pelengaris *et al*., 2002).

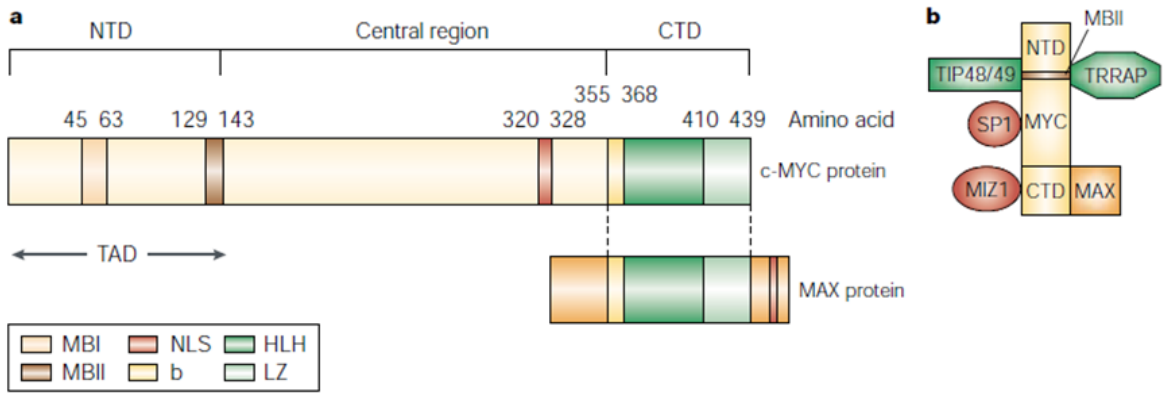

Figure 1-5: Functional domains of human c-MYC protein. a) The carboxy-terminal domain (CTD) with its basic (b) helix–loop–helix (HLH) leucine zipper (LZ) motif and MYC–MAX heterodimers. **b)** c-MYC interacting proteins (Pelengaris *et al*., 2002).

MYC boxes I and II are surrounded by regions that encompass domains involved in transactivation and transrepression (Patel *et al*., 2004). The negative partners Mad1, Mxi1, Mad3, Mad4 and Mnt also compete with MYC for MAX, dimerize with MAX and bind to identical DNA sequences in target genes. Unlike that of MYC the negative MAX dimerizing partners repress the transcription of target genes through their associations with the general transcriptional corepressors such as Sin3a/3b, through a Sin3-interaction domain (SID) and Sin3-associated histone deacetylases (HDACs) (Meyer and Penn, 2008; Pelengaris *et al*., 2002).

In contrast to the tightly regulated *c-MYC* gene in normal cells, which is only active when cells divide, deregulated expression of *c-MYC* is frequently observed in cancer cells (Schmidt, 2004). This enhances uncontrolled proliferation and metastasis of cancer cells (Allen *et al*., 2011; Dang, 1999). The *c-MYC* proto-oncogene encodes the c-MYC transcription factor, and was originally discovered in Burkitt's lymphoma as the cellular homologue to the viral oncogene (v-*MYC*) of the avian myelocytomatosis retrovirus (Pelengaris *et al*., 2002). Deregulated expression of *c-MYC* has been linked to several human cancers, and is often correlated with aggressive, poorly differentiated tumours. Such cancers include breast cancer, colon cancer, cervical cancer , small-cell lung carcinomas, osteosarcomas, glioblastomas, melanoma and myeloid leukaemias (Pelengaris *et al*., 2002; Zhang *et al*., 2010).

Moreover, *c-MYC* proto-oncogene is one of the most frequently activated oncogenes, and is estimated to be involved in 70% of human cancers (McMahon, 2010; Meyer, and Penn, 2008; Nilsson and Cleveland, 2003; Skoudy *et al*., 2011), accounting large number of cancer deaths per year. Specifically, *c-MYC* overexpression was detected in over 45% of the gastric cancer cases and it is associated with a poor clinical course of gastric cancer (Zhang *et al*., 2010). Both intestinal and diffuse-types of gastric adenocarcinoma display high *c-MYC* expression, which is associated with the occurence of metastasis (Zhang *et al*., 2010). Moreover, a high level of *c-MYC* expression in gastric cancer is associated with poor survival, indicating that *c-MYC* expression may represent an aggressive phenotype of gastric cancer (Han *et al*., 1999). Overexpression of *c-MYC* gene has also been seen in early gastric cancer when tumor invasion is confined to the mucosa or submucosa regardless of the presence of lymph node metastasis (Milne *et al*., 2007). It has been also noticed that c-MYC protein expression increased progressively from chronic active gastritis, gastric ulcer, and mild nonclassic proliferation to progressive gastric cancer, further confirming that c-MYC is involved in the routes of gastric carcinogenesis and could be an important target for treatment of gastric cancer (Busuttil and Boussioutas, 2009; Lan *et al*., 2003).

1.7. Aims of this study

Gastric cancer is featured by extremely poor prognosis with a 5 year survival rate of less than 20%, which is mainly attributed to delayed detection and lack of efficient treatment options (Jemal *et al*., 2007). The application of biomarker molecules which are confined to precancerous lesions and tumor tissues represents probably an important tool to improve the accuracy and efficiency of endoscopic gastric cancer detection. Todate, the only therapeutic option with curative potential for gastric cancer is complete resection at local stage of the tumor (Wacheck, *et al*., 2006). Gastric cancer at advanced stage remains an incurable disease due to high chemoresistance. Therefore, the two major aims of this study were to identfy potential biomarker genes for early detection of precancerous and cancerous lesions in the stomach and to develop novel therapeutic strategies for gastric cancer.

2. Materials

2.1. Technical equipments

Table 2-1: Technical equipments used in this study.

Device	Source
Analytical balance BP 610	Sartorius AG, Göttingen
Analytical balance A 120 S	Sartorius AG, Göttingen
Analytical balance Kern AGB	Gottlieb Kern & Sohn GmbH, Balingen-Frommern
ASP300 tissue protector	Leica Microsytems GmbH, Wetzlar
Avanti® J25 centrifuge	Beckman Coulter Inc., Brea, CA, USA
AxioCam HRC	Carl Zeiss AG, Oberkochen
AxioCam MRc	Carl Zeiss AG, Oberkochen
Axiophot epifluorescence microscope	Carl Zeiss AG, Oberkochen
Centrifuge 5417R	Eppendorf AG, Hamburg
Centrifuge Rotina 46R	Andreas Hettich GmbH & Co.KG, Tuttlingen
CO_2 incubator HERAcell®	Heraeus Instruments GmbH, Osterode
Cryostat Microm HM 560	Thermo Fisher Scientific, Inc., Waltham; MA, USA
Dewar carrying flask, type B	KGW-Isotherm, Karlsruhe
Digital CCD camera ORCA II-ER-1394	Hamamatsu, Hersching
Electrophoresis power supply Power Pac 200	Bio-Rad Laboratories GmbH, München
Elisa plate reader Anthos 2001	Anthos Mikrosysteme GmbH, Krefeld
Eppendorf 5432 mixer	Eppendorf AG, Hamburg
Ethilon 5-0	Ethicon, Johnson & Johnson Medical GmbH. Noderstedt
FACS Calbrator/ Flowjow software	Treestar Inc., Ashland, OR, USA
Gel doc XR+ documentation system	Bio-Rad Laboratories GmbH, München
Glass ware, Schott Duran®	Schott AG, Mainz

Heated paraffin embedding module EG1150 H	Leica Microsytems GmbH, Wetzlar
Hemocytometer (Neubauer improved)	LO-Laboroptik GmbH, Bad Homburg
HeraSafe biological safety cabinet	Thermo Fisher Scientific Inc., Waltham, MA, USA
Homogenizer silent crusher M with tool 6F	Heidolph Instruments GmbH, Schwabach
Horizontal gel electrophoresis system	Biozym Scientific GmbH, Hessisch Oldenburg
Incubator shaker thermoshaker	C.Gerhardt GmbH & Co. KG, Königswinter
Leica EG 1150 H embedding system	Leica Microsytems GmbH, Wetzlar
Magnetic stirrer Ikamag®	IKA-Werke GmbH & Co. KG, Staufen
MicroAmp optical 96 well reaction plate	Applied bisystems, Inc., Carlsbad, CA, USA
Microcentrifuge 5415 D	Eppendorf AG, Hamburg
Microliter syringe	Hamilton Bonaduz AG, Bonaduz, Switzerland
Microscope Axiovert 25	Carl Zeiss AG, Oberkochen
Microscope DM LB	Leica Microsytems GmbH, Wetzlar
Microtome Microm HM355S	Thermo Fisher Scientific Inc., Waltham, MA, USA
Microwave	Siemens, München
Mighty Small II Western blot system	Hoefer Inc., Holliston, MA, USA
Mini centrifuge MCF-2360	LMS Consult GmbH & Co. KG, Brigachtal
Mini-PROTEAN®Tetra cell	Biorad Laboratories-GmbH, München
Multipipette® stream	Eppendorf AG; Hamburg
Odyssey® Infrared imaging system	LI-COR Bioscience Corporate, Lincoln, NE, USA
Paraffin tissue floating bath microm SB80	Thermo Fisher Scientific Inc., Waltham, MA, USA
pH-Meter	WTW GmbH, Weilheim
Pipetus®	Hirschmann Laborgeräte GmbH&CoKG, Eberstadt
Power supply E844, E822, EV243	Consort, Turnhout, Belgium
Spectrophotometer NanoDrop-1000	PEQLAB Biotechnologie GmbH, Erlangen
StepOnePlus™ Real-Time PCR system	Applied Biosystems Inc., Carlsbad, CA, USA
Stereomicroscope Stemi SV 11	Carl Zeiss AG, Oberkochen

Thermocycler T1	Biometra GmbH, Göttingen
Thermocycler TGradient	Biometra GmbH, Göttingen
Thermomixer compact	Eppendorf AG, Hamburg
Tissue processor ASP300	Leica Microsystems GmbH,Wetzlar
VacuGene pump	GE Healthcare Europe GmbH, Freiburg
Vortex Reax 2000	Heidolph Instruments GmbH, Schwabach
Vortex VF2	IKA-Werke GmbH, Staufen
Water bath 1003	GFL Gesellschaft für Labortechnik GmbH, Burgwedel
Zeiss LSM 510	Carl Zeiss AG, Oberkochen

2.2. Disposables

Table 2-2: Disposables used in this study.

Disposable	Source
Cuvettes	Greiner Bio-One GmbH, Frickenhausen
Amersham Hybond™-N membrane	GE Healthcare Europe GmbH, Freiburg
Amersham illustra ProbeQuant™ G-50 Micro columns	GE Healthcare Europe GmbH, Freiburg
Cell culture plastics	BD Biosciences, Franklin Lakes, NJ, USA; TPP Tissue Culture Labware, Trasadingen, CH
Cell scraper	TPP Tissue Culture Labware, Trasadingen, CH
Chromatography paper	Whatman plc, Kent, UK
Cover slips	Menzel-Gläser, Braunschweig
Combitips Biopur®	Eppendorf AG, Hamburg
15 ml conical tubes	TPP Techno plastic Products AG, Trasadingen, Schweiz
50 ml conical tubes	Sarstedt AG, Nümbrecht
Cryotubes™	Nunc Brand Products, Napeville, IL, USA
Feather disposable scalpel	Feather Safety Razor Co., Ltd., Osaka, Japan

Glass slides Superfrost® plus	Gerhard Menzel, Glassbearbeitungswerk GmbH & Co. KG, Braunschweig
Immobilon transfer membrane	Millipore Corporate, Billerica, MA, USA
Protran BA 83 nitrocellulose	Whatman GmbH Dassel, Germany
Kodak BioMax MS film	Sigma-Aldrich Chemie GmbH, Steinheim
MicroAmp® Optical 96-Well reaction plate	Applied Biosystems Inc., Carlsbad, CA, USA
Microtome blades S35	Feather Safety Razor Co., Ltd., Osaka, Japan
PCR reaction tubes	Eppendorf AG, Hamburg
Petri dishes	Sarstedt AG, Nümbrecht
Pipet tips	Sarstedt AG, Nümbrecht
Round-bottom polystyrene tubes	Sarstedt AG, Nümbrecht
1.5 and 2 mL Reaction tubes	Eppendorf AG, Hamburg
Safe seal pipet tips, professional	Biozyme Scientific GmbH, Hessisch Oldenburg
Safe-lock reaction tubes BioPur®	Eppendorf AG, Hamburg
Serological pipettes	BD Biosciences, Franklin Lakes, NJ, USA
Single use needles Sterican® 27 gauge	B. Braun Melsungen AG, Melsungen
Single use syringes Omnifix®	B. Braun Melsungen AG, Melsungen
Sterile pipet tips	Biozym Scientific GmbH, Hessisch Oldendorf
Wound clips	MEDICON eG, Tuttlingen
Tissue embedding cassette system	Medite GmbH, Burgdorf
5 ml polystyrene round-bottom tube	BD Biosciences, Franklin Lakes, NJ, USA

2.3. Chemicals, reagents and enzymes

Restriction endonucleases were obtained from New England Biolabs (Frankfurt).

Table 2-3: Chemicals, reagents and enzymes used in this study.

Reagent/Enzyme	Source

1,4-Dithiothreitol (DTT)	Carl Roth GmbH, Karlsruhe
2log DNA Ladder	New England Biolabs, Frankfurt
3-(4,5-deimethylthiazol-2-yl)-2,5-diphenyl tetrazolium bromide (MTT reagent)	Carl Roth GmbH, Karlsruhe
5-Bromo-2´-Deoxyuridine (BrdU)	Sigma-Aldrich Chemie GmbH, Steinheim
Agarose	PEQLAB Biotechnologie GmbH, Erlangen
Ammonium per sulfate (APS)	Sigma-Aldrich Chemie GmbH, Steinheim
Ampicillin (100 mg/mL)	Carl Roth GmbH, Karlsruhe
Bis Benzamide (H33258)-Hoechst reagent	Sigma-Aldrich Chemie GmbH, Steinheim
Bovine Serum Albumin (BSA) standard	Thermo Fisher Scientific, Piece Biotechnology, Rockford, IL, USA
Bradford reagent	Serva Electrophoresis GmbH, Heidelberg
Bromphenol blue	Sigma-Aldrich Chemie GmbH, Steinheim
Chloramphenicol	Applichem, Darmstadt
Chloroform	Carl Roth GmbH, Karlsruhe
Complete, EDTA-free, protease inhibitor cocktail tablets	Roche Deutschland Holding GmbH, Grenzach-Wyhlen
Dimethylsulfoxid (DMSO)	Carl Roth GmbH, Karlsruhe
DNAse I	Qiagen GmbH, Hilden
dNTP mix, 10mM each	Fermentas GmbH, St. Leon-Rot
Dodecylsulfate Na-salt in pellets (SDS)	Serva Electrophoresis GmbH, Heidelberg
Dulbeco`s phosphate buffered saline (PBS)	Biochrom AG, Berlin
Ethanol	Carl Roth GmbH, Karlsruhe
Ethidiumbromide	Carl Roth GmbH, Karlsruhe
Formaldehyde	Sigma-Aldrich Chemie GmbH, Steinheim
Gel loading dye, blue	New England Biolabs GmbH, Frankfurt am Main
Glycerol	Sigma-Aldrich Chemie GmbH, Steinheim
Glycin	Carl Roth GmbH, Karlsruhe

HEPES	Sigma-Aldrich Chemie GmbH, Steinheim
HotStarTaq DNA Polymerase	Qiagen GmbH, Hilden
Hydrochloric acid (HCl)	Carl Roth GmbH, Karlsruhe
Isofluran Forene	Abbott GmbH, Wiesbaden
Isopropanol	Carl Roth GmbH, Karlsruhe
Kanamycin (100mg/mL)	Carl Roth GmbH, Karlsruhe
LB Agar and Broth Luria/Miller	Carl Roth GmbH, Karlsruhe
Magnesium chloride	Carl Roth GmbH, Karlsruhe
Metacam	Boehringer Ingelheim Pharma GmbH, Ingelheim am Rhein
Methanol	Carl Roth GmbH, Karlsruhe
NaOH	Carl Roth GmbH, Karlsruhe
Non-fat dry milk blotting grade blocker	Bio-Rad Laboratories GmbH, München
Nonidet NP-40	Sigma-Aldrich Chemie GmbH, Steinheim
Novalgin	Sanofi-Aventis Deutschland GmbH, Frankfurt am main
Odyssey blocking reagent	LI-COR Corp. Offices, Lincoln, NE, USA
PEI transfection reagent	PEQLAB
Phosphatase inhibitor Set	Roche Deutschland Holding GmbH, Grenzach-Wyhlen
PI-103	Selleck Chemicals LLC, Houston, TX, USA
Power SYBR® Green PCR master mix	Applied Biosystems Inc., Carlsbad, CA, USA
Precision plus protein™ all blue standard	Bio-Rad Laboratories GmbH, München
ProSense® 750 flourescent imaging probe	Perkinlmer, Inc. Boston, USA
Protease Inhibitor Set	Roche Deutschland Holding GmbH, Grenzach-Wyhlen
Proteinase K, recombinant, PCR grade	Roche Deutschland Holding GmbH, Grenzach-Wyhlen
Proteinase K	Roche Deutschland Holding GmbH, Grenzach-Wyhlen

RDD	Qiagen GmbH, Hilden
REDTaq® ReadyMix™ PCR reaction mix	Sigma-Aldrich Chemie GmbH, Steinheim
Restriction endonucleases	New England Biolabs GmbH, Frankfurt am Main
RNaseA	Fermentas GmbH, St. Leon-Rot
RNAse-free DNase set	Qiagen GmbH, Hilden
Rotiphorese® Gel 30	Carl Roth GmbH, Karlsruhe
S.O.C. medium	Invitrogen GmbH, Karlsruhe
SuperScript II reverse transcriptase	Invitrogen GmbH, Karlsruhe
T4 DNA ligase	Invitrogen GmbH, Karlsruhe
TE buffer, pH8.0	AppliChem GmbH, Darmstadt
TEMED	Carl Roth GmbH, Karlsruhe
Tissue Tek® O.C.T™ compound	Sakura Finetek Europe B.V, Alphen aan den Rijn, Netherlands
Tris hydrochloride (TrisHCl)	Carl Roth GmbH, Karlsruhe
TritonX-100	Merck KGaA, Darmstadt
Tween-20	Carl Roth GmbH, Karlsruhe
β-Mercaptoethanol	Sigma-Aldrich Chemie GmbH, Steinheim

2.4. Kits

Table 2-4: Kits used in this study.

Kit	Source
RNeasy Mini kit	Qiagen GmbH, Hilden
QIAmp DNA mini kit	Qiagen GmbH, Hilden
QIAprep® spin miniprep kit	Qiagen GmbH, Hilden
QuantiFast SYBR green PCR kit	Qiagen GmbH, Hilden
TaqMan® reverse transcription kit	Applied Biosystems Inc., Foster City, CA, USA
Zero Blunt® TOPO® PCR cloning kit reagents	Invitrogen GmbH, Karlsruhe
Magnetic simple ChIP enzymatic chromatin	Cell Signalling Technology, Inc, Danvers, MA,

IP Kit	USA
FITC Annexin V apoptosis detection kit I	BD Biosciences, Franklin Lakes, NJ, USA

2.5. Antibodies

Table 2-5: Antibodies used in this study.

Antibody	Source	Application
BCL_{XL} made in rabbit Cat#2762S	Cell Signalling Technology, Inc, Danvers, MA, USA	Western blot
c-MYC made in rabbit Cat#475956	Cell Signalling Technology, Inc, Danvers, MA, USA	Western blot
Mouse anti cleaved-PARP (Asp214) MAb, Cat# 519000017	BD Biosciences, Franklin Lakes, NJ, USA	Western blot
Hif-α1 (H-206) rabbit polyclonal IgG Cat#sc-10790	Santa Cruz Biotechnology Inc., Santa Cruz, CA, USA	Western blot
MCL1 (s-19) rabbit polyclonal IgG Cat#sc-819	Santa Cruz Biotechnology Inc., Santa Cruz, CA, USA	Western blot
p65 (c-20) rabbit polyclonal IgG Cat# sc-372	Santa Cruz Biotechnology Inc., Santa Cruz, CA, USA	Western blot
STAT3 made in rabbit Cat#9132	Cell Signalling Technology, Inc, Danvers, MA, USA	Western blot
Anti-β-Actin (produced in mouse) Cat#A5316	Sigma-Aldrich Chemie GmbH, Steinheim	Western blot
Anti-mouse cathepsin S made in goat, Cat#AF1183	Research & Diagnostics Systems, Inc. (R&D Systems), USA	Immunohistochemistry
Anti-mouse cathepsin L made in goat,Cat#AF952	Research & Diagnostics Systems, Inc. (R&D Systems), USA	Immunohistochemistry
Anti-mouse cathepsin H made in goat, Cat#AF1013	Research & Diagnostics Systems, Inc. (R&D Systems), USA	Immunohistochemistry
Anti-mouse cathepsin B made in goat, Cat#AF965	Research & Diagnostics Systems, Inc. (R&D Systems), USA	Immunohistochemistry
Anti-mouse MMP3 (c-19) made in goat, Cat#Sc-6839	Research & Diagnostics Systems, Inc. (R&D Systems), USA	Immunohistochemistry

Anti-mouse MMP2(Ab-3) made in goat, Cat#IM33	Research & Diagnostics Systems, Inc. (R&D Systems), USA	Immunohistochemistry
Anti-eIF4E made in mouse Cat#610269	BD transduction laboratories	Western blot
AlexaFluro® 680 goat anti-mouse IgG (H+L) highly cross-adsorbed Cat#A21058	Invitrogen GmbH, Karlsruhe	Western blot
AlexaFluro® 680 goat anti-rabbit IgG (H+L), Cat#A21076	Invitrogen GmbH, Karlsruhe	Western blot
AlexaFluro® 750 goat anti-mouse IgG (H+L) highly cross-adsorbed Cat#A21037	Invitrogen GmbH, Karlsruhe	Western blot
AlexaFluro® 750 goat anti-rabbit IgG (H+L), Cat#A21039	Invitrogen GmbH, Karlsruhe	Western blot

2.6. Primers

All primers applied in this study were synthesised by MWG (sequencing and qPCR Primers). Unless otherwise stated all primers in the list were applied for qPCR.

Table 2-6: Human primer sets applied in qPCR.

Gene	Primer name	Primer sequence (5' - 3')
PPIA	Cyc-FW	ATGGTCAACCCCACCGTGT
	Cyc-RV	TCTGCTGTCTTTGGGACCTTGTC
MCL1-L	MCL1L-FW	GCATCGAACCATTAGCAGAAAG
	MCL1L-RV	AAAGCCAGCAGCACATTCC
c-MYC	c-MYC-FW1317	AGCGACTCTGAGGAGGAACA
	c-MYC-RV 1403	CTCTGACCTTTTGCCAGGAG
EIF4E	eIF4EFWTaq	ACAAGTCAGTCTGAAACCATCGAAC
	eIF4ERVTaq	CTTCATCCTCTTCGGCCACTCCTCC
BCL_{XL}	BCL_{XL} FW	CCACTTACCTGAATGACCACCTAGA
	BCL_{XL} RV	GCTGCATTGTTCCCATAGAGTTC
MMP9	MMP9-FW	GCACCACCACAACATCACCTAT
	MMP9-RV	TGTACACGCGAGTGAAGGTGAG

MMP13	MMP13-FW	TCCCAGTGGTGGTGATGAAGA
	MMP13-RV	GGATTCCCGCGAGATTTGTAG
MMP2	MMP2 -FW	CCTGAGATCTGCAAACAGGACAT
	MMP2-RV	GCCAAATGAACCGGTCCTT
MMP3	MMP3-FW	ACCTGGAAATGTTTTGGCCCAATGC
	MMP3-RV	GGTCCCTGTTGTATCCTTTGT
CTSB	CTSB- FW	CTGTCGGATGAGCTGGTCAACT
	CTSB -RV	CCACCCAGGAAGGTACCACATA
CTSL	CTSL-FW	CTGTTTTATGAGGCCCCCAGA
	CTSL-RV	GCCCAACAAGAACCACACTGAC
CTSS	CTSS-FW	TCGACTCAGACGCTTCCTATCC
	CTSS-RV	TGAACATGTGGCAGCACGAT
CTS H	CTS H_FW	TGGTTATTGCAAGTTCCAACC
	CTS H-RV	GTGACTCAGGACTTCATGATG
MCL1-587	MCL1-587-RV	ACGGGGAAGGTTCAGTGATGG
	MCL1-587-FW	TTAGGGTAGCACGTGGAGCA
eIF4E-75	eIF4E-75FW	TACTCACGCAGCCGCAGTC
	eIF4E-75RV	TCGCACAACCGCTCCAG
PPIA-377	PPIA377FW	GCGACCTTGAGGCCTGCGTT
	PPIA377RV	CGGCTCTTCGGCCGTTGTCA
MCL1-13kb3’	MCL1-13kb3´FW	GCTGTGCTGAGAGGCCTGGG
	MCL1-13kb3´RV	AGCACACAAACATGCCGACCC
*eIF4E*16kb3’	eIF4E16kb3´FW	AATGCAGGGTGGGGTTGCTCA
	eIF4E16kb3´FW	GCCCAGGGCTGGTCTTGACCT
Mycoplasma primer	MycoFW	GGGAGCAAACAGGATTAGATACCCT
	MycoRV	TGCACCATCTGTCACTCTGTTAACCTC

Table 2-7: Murine primer sets applied in qPCR.

Target name	Primer name	Sequence (5' - 3')
MMP9	MMP9-FW	AAGACGACATAGACGGCATC
	MMP9-RV	ATAGGCCGTGGGAGGTATAG
MMP13	MMP13-FW	TGGACCTTCTGGTCTTCTGG
	MMP13-RV	CTCATGGGCAGCAACAATAA
MMP2	MMP2 -FW	ACACTGGGACCTGTCACTCC
	MMP2-RV	TGTCACTGTCCGCCAAATAA
MMP3	MMP3-FW	CAGACTTGTCCCGTTTCCAT
	MMP3-RV	GGTGCTGACTGCATCAAAGA
CTSB	CTSB- FW	GGAGATACTCCCAGGTGCAA
	CTSB -RV	CTGCCATGATCTCCTTCACA
CTSL	CTSL-FW	TCAGTGAGATCAGTTTGCCG
	CTSL-RV	TCCCTCAGTGCTCAGAACCT
CTSS	CTSS-FW	ACCATTGGGATCTCTGGAA
	CTSS-RV	CAGATGAGACGCCGTACTTC
CTS H	CTS H_FW	CCAGTGGGAAAATGCTGTCT
	CTS H-RV	TCCATGATGCCCTTGTTGTA
PPIA	Cyclo-FW	ATGGTCAACCCCACCGTGT
	Cyclo-RV	TTCTTGCTGTCTTTGGAACTTTGTC

2.7. siRNAs

Table 2-8: siRNAs used in this study.

Designation	Oligo name	5'-3' sequence (sense)
siMCL1#1	siMCL1-hu-+145_01	AAGAAACGCGGUAAUCGGACU
siMCL1#2	siMCL1-hu_02	CGCCGAAUUCAUUAAUUUA
siBCL_{XL}	hBCL_{XL}	GGAGAUGCAGGUAUUGGUG
sip65	sip65+144	GAUCAAUGGCUACACAGGA

siSTAT3	siSTAT3	CAUCUGCCUAGAUCGGCUA
siMYC#1	siMYC+87	CUUCUACCAGCAGCAGCAG
siMYC#2	Si-c-MYC-2	GAACACACAACGUCUUGGA
sieIF4E#1	Hu-eIF4E1	GGACGAUGGCUAAUUACAU
sieIF4E#2	Hu-eIF4E1	GGAUGGUAUUGAGCCUAUG

2.8. Inhibitors

Table 2-9: Inhibitors used in this study.

Inhibitor	Source
c-Myc inhibitor (10058-F4)	Calbiochem, EMD Chemicals Inc., Darmstadt, Germany
Suberoylanilide hydroxamic acid (SAHA)	LC Laboratories
4SC-201	4SC AG, Germany
4SC-202	4SC AG, Germany

2.9. Bacterial strains

Table 2-10: Bacterial strains used in this study.

Bacterial strain	Source
One Shot® TOP10 chemically competent bacteria	Invitrogen GmbH, Karlsruhe

2.10. Buffers and solutions

All buffers are prepared with bidistilled H_2O.

Table 2-11: Buffers and solutions used in this study.

Buffer	Compositions
KCM Buffer	500 mM KCl
	150 mM $CaCl_2$
	250 mM $MgCl_2$
Glycerol stock solution	65% Glycerol
	0,1 M $MgSO_4$

	25mM Tris HCl pH=8
Loading Buffer Orange G (6x)	60% (v/v) Glycerol
	60 mM EDTA
	0.24% (w/v) Orange G
	0.12% (w/v) SDS
IP buffer pH 7,9	50 mM HEPES
	150 mM NaCl
	1 mM EDTA
	0,5% NP-40
	10% Glycerol
	1% phosphatase inhibitor (add prior to use)
	1% protease inhibitor (add prior to use) pH adjusted to 7,9
Collection gel buffer	0,5 M Tris,pH adjusted to 6.8 with HCl
Seperation gel buffer	1,5 M Tris , pH adjusted to 8,8 with HCl
Running buffer	25mM TrisHCl
	192 mM Glycin
	0,1% SDS
Transfer buffer (semi-dry)	25 mM TrisHCl
	192 mM Glycin
	0,1% SDS
	20% Methanol pH adjusted to 8,3
Transfer buffer (wet blot)	25mM Tris,192mM Glycin, 20% Methanol
5x protein loading buffer pH 6,8	10% SDS
	50% Glycerol
	228 mM TrisHCl
	0,75 mM bromphenol blue
	5% β-Mercaptoethanol

Tris buffered saline (TBS)	0.5M Tris, 1.5M NaCl pH adjusted to 7.6
PBS pH 7,4	20 mM Na_2HPO_4
	50 mM NaCl
50x TAE-Buffer pH 8,5	2 M TRIS
	100 mM EDTA
	5, 71% (v/v) Acetic acid (100%)

2.11. Histochemistry reagents

Table 2-12: Histochemistry reagents used in this study.

Histochemistry reagent	Source
Avidin/Biotin blocking Kit	Vector Laboratories, Burlingame, CA, USA
Biotinylated anti-mouse IgG (H+L)	Vector Laboratories, Burlingame, CA, USA
Biotinylated anti-rabbit IgG (H+L)	Vector Laboratories, Burlingame, CA, USA
Biotinylated anti-goat IgG (H+L)	Vector Laboratories, Burlingame, CA, USA
Vectashield® mounting medium with DAPI	Vector Laboratories, Burlingame, CA, USA
Citric acid based antigen unmasking solution	Vector Laboratories, Burlingame, CA, USA
DAB Peroxidase Substrate Kit	Vector Laboratories, Burlingame, CA, USA
Eosin	Waldeck GmbH, Münster
Goat serum G9023	Sigma-Aldrich Chemie GmbH, Steinheim
Hydrogen per Oxide (H_2O_2) 30%	Merck KgaA, Darmstadt
Haematoxylin	Merck KgaA, Darmstadt
Histoclear	Carl Roth GmbH, Karlsruhe
Rabbit serum R9133	Sigma-Aldrich Chemie GmbH, Steinheim
Roti® Histofix (4% Formalin)	Carl Roth GmbH, Karlsruhe
VECTASTAIN® Elite ABC solution	Vector Laboratories, Burlingame, CA, USA

2.12. Cell Culture

A panel of human and murine gastric cancer cell lines was used in this study. Except for MGC4 and MGC8 (which are of murine origin) all of the other cell lines are of human gastric cancer origin.

Table 2-13: Cell lines used in this study.

Cell line	Source
HSC45-M2	Kind gift from Dr. Senekowitsch-Schmidtke
KATO-III	American type culture collection (ATCC)
MGC4	kind gift from Dr. W. Zimmermann
MGC8	kind gift from Dr. W. Zimmermann
MKN45	kind gift from Dr. R.Mejías-Luque
AGS	DSMZ
ST23132	kind gift from Dr. R.Mejías-Luque
NUGC4	kind gift from Dr. R. Mejías-Luque
ST2957	kind gift from Dr. R. Mejías-Luque

2.13. Cell culture, reagents and media

Table 2-14: Used reagents for cell culture.

Reagent	Source
Fetal Calf serum (FCS)	Biochrom AG, Berlin
L-Glutamin	Invitrogen GmbH, Karlsruhe
Non essential amino acids (100x)	Invitrogen GmbH, Karlsruhe
Sodiumpyruvat	Invitrogen GmbH, Karlsruhe
PBS	Invitrogen GmbH, Karlsruhe
Penicillin-Streptomycin solution	Invitrogen GmbH, Karlsruhe
Dulbeco´s modified eagle medium (D-MEM) with L glutamine	Invitrogen GmbH, Karlsruhe
L-Glutamine (100X)	Invitrogen GmbH, Karlsruhe
RPMI 1640 medium	Invitrogen GmbH, Karlsruhe

Sodium pyruvate MEM	Invitrogen GmbH, Karlsruhe
Freezing Medium	7 % D-MEM, 2% FCS, 1%DMSO

3. Methods

3.1. Animal Experiments

The *CEA-TAG* mouse model was generated and kindly provided by Prof. Zimmermann (Thompson *et al*., 2000) and applied in this study for imaging gastric cancer with the aid of “smart” probes. The expression pattern of cathepsins and matrix metalloprotinases (MMPs) as potential biomarker molecules for preneoplastic lesions and early gastric cancer detection was determined in the stomach tissues of these mice. For *ex vivo* imaging of gastric cancer in these mice, 150µl prosense-750 probe was injected intravenously (i.v.) and the mice were kept back to their cage for 24 hours. After 24 hrs of i.v injection, the mice were killed and the stomach was carefully removed, contents were washed with PBS and near-infrared fluorescent (NIRF) imaging was performed on a planar Odyssey scanner at 800 nm. Afterwards, *ex vivo* histological analysis was performed (as described in section 3.2). All animal studies conducted meet the requirements of the European guidelines for the care and use of laboratory animals and were approved by the local authorities.

3.2. Histological analysis and stainings

3.2.1. Paraffin sections

Stomach tissue was washed with PBS, fixed in Roti® Histofix for 24 h, dehydrated using ASP300 Tissue Processor (Leica) and embedded in paraffin. A series of 4 µm thick sections were cut for stainings.

3.2.2. Haematoxylin and eosin (HE) staining

Wax was removed from paraffin embedded tissue sections with the aid of 2x Roti® Histol (Carl Roth) for 5 minutes. Then, the tissue was rehydrated with the decreasing alcohol series (2x 100%, 2x 98% and 2x 80% EtOH), each for 3 minutes. Sections were then stained in haematoxylin for 5 sec, gently washed in tap water for 10 min and then stained in eosin for approximately 20 sec. Tissue was dehydrated with an increasing alcohol series (2x 80%, 2x 96% and 2x100% ethanol). After immersing 2x for 5 min in Roti® Histol (Carl Roth) slides were mounted in Pertex.

3.2.3. Immunohistochemistry

The stomach tissue was rehydrated after de-paraffinizing the embedded stomach tissue sections. Microwave antigen retrieval was performed using unmasking solution (Vector Labs) for 9 min. After a cooling period of at least 15 min, slides were washed in distilled H_2O. Endogenous peroxidase reactivity was blocked by incubating slides in 3% H_2O_2 for 20 min. After washing with water and PBS for one and two times, respectively, incubation with 5% serum in PBS for 1 h was carried out to block unspecific antibody binding. Primary antibody was diluted to desired concentration in 3% serum in PBS and incubated. In all cases, the primary antibody was diluted to a factor of 1:500, goat serum was used for blocking and incubation was for 1 h at room temperature (RT). The slides were washed three times with PBS to remove unspecifically bound primary antibody. Biotinylated secondary antibody was diluted (1:200) and incubated for 1 h at RT. After washing, VECTASTAIN® Elite ABC solution (Vector Labs) was added and afterwards slides were incubated with 3, 3'-diaminobenzidine tetrahydrochloride (DAB, Vector Labs) until suitable brown staining is developed. Slides were finally counterstained with hematoxylin and mounted in pertex.

3.3. Cell Culture conditions and preservation of cells

A panel of 6 human gastric cancer cell lines: AGS, HSC45-M2, KatoIII, ST2957, MKN47, ST23132, NUGC4 and 2 murine gastric cancer cell lines: MGC4 and MGC8 (stated in table 2-13) were applied in this study. All of the cell lines were cultured at 37°C and 5% CO_2, regardless of their origin of generation. The required media composition for all human origins was the same (500ml DMEM media, 10% FCS, 1% P/S) but the murine origins need different compositions (500ml DMEM media, 10% FCS, 1% P/S, 1% NEAA and 1% sodium pyruvate). All cell culture work was conducted in a sterile laminar flow bench.

To subculture, cells were washed with sterile PBS in a laminar flow hood, trypsinated for 1-5 min at 37°C and passaged in a new flask containing fresh medium. For cryopreservation, the trypsinated cells were suspended in fresh medium and centrifuged at 1000 rpm for 5 min. The supernatant was discarded carefully, the pellet was resuspended in ice-cold freezing medium and kept in liquid nitrogen for further use.

3.4. Molecular techniques

3.4.1. Transformation of competent bacteria and isolation of plasmid DNA

KCM method was applied to transform Top 10 chemically competent bacteria. Very briefly, 200-500 ng of plasmid DNA were diluted in 100 µL 1x KCM buffer and mixed with 100 µL of One Shot® TOP10 chemically competent bacteria (Invitrogen). Reactions were kept at 4°C for 20 min and at RT for 10 min. After addition of 1 mL of S.O.C medium (Invitrogen) the bacteria were incubated on a horizontal shaker at 25 or 37°C for 1 or 2 h based on optimal growth temperature of the bacteria. Transformed cells were then streaked onto agar plates containing the appropriate antibiotic for selection at various dilutions and incubated over night at 37°C. Before amplification of plasmids, correct cloning was confirmed with screening PCR. A glycerol stock for preservation was made by mixing equal volumes of glycerol stock solution and freshly grown bacteria (storage –80°C). Based on the amount of plasmid DNA needed Qiagen Plasmid Mini Kit was used according to manufacturer's protocol. Verification of intact and correct plasmid was done by digestion with restriction endonucleases followed by agarose gel electrophoresis.

3.4.2. Screening potential biomarker genes for imaging gastric cancer

To investigate the expression levels of MMPs and cathepsins in human and murine gastric cancer cell lines, the corresponding gastric cancer cell lines were cultured, total RNA was extracted and reverse transcribed to cDNA. Then, qPCR was carried out. Similarly, to compare the mRNA expression pattern of cathepsins and MMPs in normal and tumour tissues from murine stomach, murine stomach was removed and washed with PBS. The stomach was macroscopically categorized into tumor region (most probably the antrum region in this case) and normal tissues (fundus/corpus described in figure 1-1). Twenty miligram of each of the categorized tissues is cut into smaller pieces, and homogenized in RLT buffer. Homogenized tissues were stored at -80°C for futher use to extract total RNA. The extracted RNA was immediately reverse transcribed into cDNA and qPCR was performed.

3.4.3. RNA isolation and quantitative PCR (qPCR)

For expression analysis of various desired target genes in murine gastric tumour cells, total RNA was isolated from murine gastric cancer cell lines that were described in table 2-13. For doing so, cells were grown to 80% confluency, washed with PBS, lysed with RLT buffer containing ß-mercaptoethanol. After scraping, the cells were collected into a BioPur safelock reaction tube and samples were stored at –80°C until further experiment. For expression analysis of the same targets in murine stomach, RNA was isolated from 20mg of murine stomach. Intact stomach tissue was placed in RLT buffer and sonified in a silent crusher. Afterwards, the same procedure as cells case was followed. Total RNA from samples in RLT buffer was isolated with RNeasy Kit and treated with DNAse I according to manufacturer's protocol. A single µg RNA per 50 µl mix were reversely transcribed using random hexamer primers, TaqMan reverse transcription reagents and SuperScript II reverse transcriptase. Finally, the reversely transcribed cDNA was stored at –20°C for further use.

Based on the manufacturer's guidelines, qPCR primers were designed using Primer Express software (Applied Biosystems). SYBR® Green PCR Master Mix and 300 nM of each primer were used to perform qPCR. Cyclophilin was used as a housekeeping gene for normalizartion of the samples. All samples were done in triplicates.

Gene expression was quantified by standard method (for Cathepsins and MMPs) and the comparative CT method with normalizing CT values to the housekeeping gene-cyclophilin A was performed in all other cases. After amplification, melting curve analysis was performed to ensure the products' specificity. To ensure experimental accuracy, all reactions were performed in triplicate. Primers were tested for efficiency before applications.

3.4.4. Protein isolation and detection

Cells were grown to 80% confluency, washed twice with ice-cold PBS, and lysed in IP-buffer and protease and phosphates inhibitors, both of the later were added at the ratio of 1:9. Lysates were scraped with cell scrapper and collected into a 1, 5ml epi tube and stored at –80°C for further application. After keeping the cell lysates in liquid nitrogen for 30 minutes, cell lysates were centrifuged at 14,000 rpm and 4°C for 25 min prior to further use. The supernatant was the total cell lysate. Supernatant was taken and protein content was determined by Bradford assay. Equivalent micro

grams of proteins from each sample were loaded per well for western blot analysis, Laemili buffer was used as a loading buffer.

3.4.5. Western blot

To perform western blot with sodium dodecyle sulphate polyacrylamide gel electrophoresis (SDS-Page) method, about 50-150 µg protein were boiled in 1x protein loading buffer and loaded into 10% or 12% polyacrylamide gel. Gels were let run at 100V or more or less as desired. Precision plus protein standards were used as a marker to control the running of the gel. Proteins were separted according to their molecular weight in the gel and immobilized on Immobilon transfer membrane (Millipore). Wet blot was performed either for 2 h at 130 V and 300mA or over night at 30 V and 90mA. After transfer is done, the membrane was washed with PBS for 5 min to clean methanol and other residues. To avoid unspecific binding of the antibody, membrane was incubated for 1 h in a 1:1 dilution of Odyssey® blocking reagent or 5% odyssey blocking skim milk in PBS at RT. Subsequently, the membrane was incubated with primary antibody for over night at 4°C. After washing three times with 1% Tween in PBS, the membrane was incubated in secondary antibody (1:2000 dilutions) for 1 h at RT shaking in the dark place. Afterwards, the membrane was washed three times for 10 minutres with 1% Tween in PBS and detection was performed in Odyssey® Infrared Imaging System.

3.4.6. siRNA transfection

Double-stranded siRNA transfection was performed with the aid of polyethylenimine (PEI) at a final concentration of 50 nM as described recently (Wirth *et al*., 2011). Briefly, 24 hrs prior to transfection different amounts of gastric cancer cells were seeded in 96-well plates (culture area, 0.328 cm2/well), or 100-mm dishes (culture area, 58.1 cm2/dish). Subsequently, the cells were washed with PBS followed by application of 80µl PEI and 9.2 ml serum-free medium. PEI stock solution was diluted in 10 and 400 µl of OptiMEM for 5 minutes to give a final ratio of (PEI stock solution to final media- volume) and 4:1000 (vol/vol). Fifty-nmol synthetic siRNA was dissolved separately in 10 or 400 µl serum-free medium. PEI and siRNA solutions were mixed and incubated together for 30 minutes. The PEI-siRNA solution was added to the adherent cells and serum-free medium was substituted by full medium 24 hours after transfection.

3.4.7. Quantitative chromatin immunoprecipitation (qChIP)

Chromatin immunoprecipitation (ChIP) were performed using magnetic SimpleChIP Enzymatic Chromatin IP Kit, according to the manufacturer's protocol. Briefly, $4X10^7$ cells were grwon in a 15 cm culture dishes in a 20 ml media. Proteins were cross linked to DNA by adding 540µl of 37% formaldehyde and incubated for 10 minutes. Two ml of 10X glycine was added to each culture dish and incubated for 5 minutes. The media was removed and cells were washed with buffers and protease inhibitors that were provided in the kit. The pellet nuclei were incubated in a 5µl micrococcal nuclease at 37°C for 20 minutes. The micorococcal nuclease digestion was hindered by adding EDTA, centrifuged and resuspended in ChIP buffer. The nuclei digestion condition was optimized and chromatine digetion and concentrations were analysed. Then, chromatin was immunoprecipitated, washed with low and high salt buffers, eluted from antibody-protein G beads and cross-links were reversed. Finally, DNA was purified and qPCR was performed. For each sample ΔCt values were calculated using ΔCt = (Ct (sample)-Ct (input)). ΔΔCt was calculated using ΔΔCt = (ΔCt (experimental sample) - ΔCt (negative control)).The fold difference between the experimental sample and the negative control (IgG) was determined as $2^{-\Delta\Delta Ct}$

3.4.8. Annexin V staining

Annexin V, conjugated to fluorochromes-FITC, is a 35-36 kDa Ca^{2+} dependent phospholipid-binding protein that has a high affinity for phospholipid phosphatidylserine (PS) and binds to cells with exposed PS. Staining with FITC Annexin V is typically used in conjunction with a vital dye such as propidium iodide (PI) to help identify different stages of apoptosis (Koopman *et al*., 1994). Approximately, $1x10^6$ cells were seeded in 10cm culture dish, treated with desired inhibitors. Cells were washed with ice cold PBS, trypsinated, collected into 50ml falcon tube, centrifuged at 1000rpm and 4^oC for 5 minutes. Then, the supernatant was discarded. Cells were washed in cold PBS twice, resuspende in 1ml binding buffer (1:10 dilution). To perform FACS analysis, 100µl of the cell suspension was mixed with 400µl of the binding buffer. Afterwards, 5µl of each Annexin/FITC and PI reagents was added into the above suspension, cells were vortexed and incubated for 15 min in dark. Finally, flow cytometry was determined within 1 hr time.

3.5. Treatment of cells with various inhibitors and viability assay

3.5.1. Treatment of cells with various inhibitors

Five thousand and 300, 000 cells were seeded in a 96 well plate and 10cm culture dishes, respectively and incubated for 24 h prior to treatment. Then, the stabilized cells were treated with desired concentrations of different inhibitors described in table 2-9. Subsequently, cells were incubated for the next 24 or 48 hrs as required, after which viability assay was carried out.

3.5.2. Viability assay

To determine cell viability, MTT (3-(4,5-Dimethylthiazol-2-yl)-2,5-diphenyltetrazolium bromide) assay was used (Mosmann, 1983). In each well of 96 well plates 10 µL MTT reagent (5 mg/mL MTT in PBS) per 100 µL media were added and plates were incubated at 37°C for 4 hrs. Media was cautiously removed with 100µl pippet tips. Cells were lysed in 200 µl of mixitures of equal volumes of DMSO: EtOH, the plates were incubated at RT with agitation for 10 min and OD600 was determined. All experiments were done in triplicates in at least three independent experiments.

Table 3-1: Dilutions of primary antibody for Western blotting.

Primary Antibody	Dilution	Secondary Antibody
Anti-ß-Actin	1:2000	Anti-mouse
Anti-c-Myc	1:500	Anti-rabbit
Anti-BCL_{XL}	1:1000	Anti-rabbit
Anti-MCL1	1:1000	Anti-rabbit
Anti- P65	1:1000	Anti-rabbit
Anti-STAT3	1:1000	Anti-rabbit
Anti-HIF-1-α	1:1000	Anti-rabbit
Anti-eIF4E	1:1000	Anti-Mouse

Table 3-2: Working concentrations of inhibitors used in this study.

Inhibitor	Working concentration range				Mode of action
SAHA	0.5 µM	1 µM	2 µM	4 µM	Pan-HDAC inhibitor
4SC-201	0.5 µM	1 µM	2 µM	4 µM	HDAC inhibitor
4SC-202	0.5 µM	1 µM	2 µM	4 µM	HDAC inhibitor
myc-I	12.5µM	25 µM	50µM	100 µM	inhibits MYC-MAX dimerization

3.5.3. Hoechst staining

The blue fluorescent Hoechst dyes are cell permeable nucleic acid stains that have great applications in testing the viability of cells (Latt *et al*., 1975) because the fluorescence of these dyes is very sensitive to DNA conformation and chromatin state in cells. Cells were grown in a 96-well plate, treated with desired inhibitor for required period of time. Briefly, 200µM stock solution of Hoechst stain was diluted (1:250) with DMEM media. Of this diluted solution, 100µl was dispensed in each well containing 100µl cell culture. Afterwards, the plate was incubated at 37°C for 15 minutes. Cells with blue stainings were considered as apoptotic ones and counted with cell counter by looking under inverted microscope equipped with UV lamp.

3.6. Statistical analysis

Graphical depictions and statistical analysis were done with GraphPad Prism5 software (La Jolla, USA). Data are presented in arithmetic mean +/- standard deviation. A two-tailed Student`s t-test was used to test statistical significance. Statstical *p*-values are indicated and a p-value of $p<0.05$ are considered as statistically significant. Inhibitor concentration 50 (IC_{50}) values were calculated with GraphPad Prism4 software.

4. Results

4.1. Early detection of gastric cancer

4.1.1. Identification of cathepsins and MMPs as potential tools for molecular imaging in gastric cancer

Cathepsins and matrix metalloprotinases (MMPs) are involved in extracellular matrix degradation (Deryugina and Quigley, 2006), tumor initiation and metastasis (Gocheva and Joyce, 2007). They are reported to be promising tools for *in vivo* molecular detection of precancerous and cancerous lesions in several cancer types (Cavallo-Medved *et al*., 2009; Eser *et al*., 2011; Mahmood and Weissleder, 2003; von Burstin *et al*., 2008). To broaden further the application of these proteins for molecular detection of precursor and cancerous lesions in gastric cancer, the expression pattern of cathepsins and MMPs in murine gastric cancer cell lines and stomach tissues was determined by qPCR. In the same fashion, the expression pattern of these proteases in human gastric cancer cell lines was detected. The results indicated that cathepsins B and H and MMP2 are overexpressed in KatoIII, AGS and HSC45-M2 cell lines (Figure 4-1 A and B). Only marginal expression of other cathepsins such as cathepsin S and L and MMPs such as MMP3, MMP9 and MMP13 was observed in human gastric cancer cell lines.

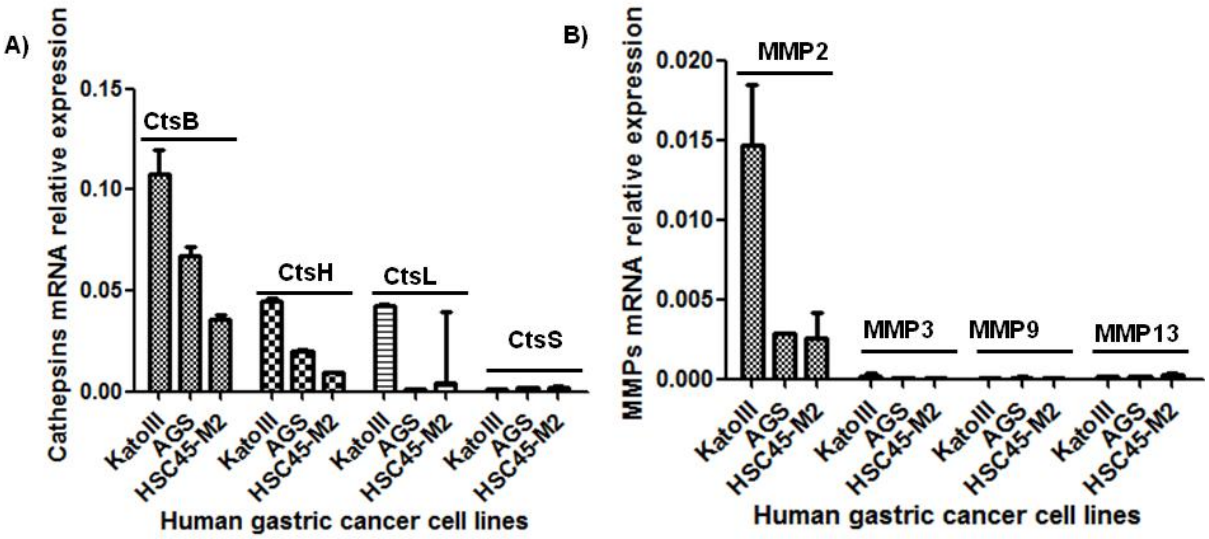

Figure 4-1: mRNA expression of cathepsin (Cts) and matrix metalloproteinases (MMPs) in human gastric cancer cell lines. Human cell lines were grown to exponential phase and total RNA was isolated, reverse transcribed and qPCR was performed to determine the level of expression of mRNAs of (A) cathepsins and (B) MMPs. Cyclophilin was used as a house keeping gene. Experiments were done in triplicates and data are presented as mean and standard error of the mean (S.E.M).

Analogous to its human counter parts, strong expression of cathepsin B was observed in murine gastric cancer cell lines (Figure 4-2A). The expression pattern of cathepsin L in human gastric cancer cells was weaker than in murine gastric cancer cell lines. MMP2 expression level showed a high standard deviation in murine cell lines, indicating tumor heterogeneity (Figure 4-2B).

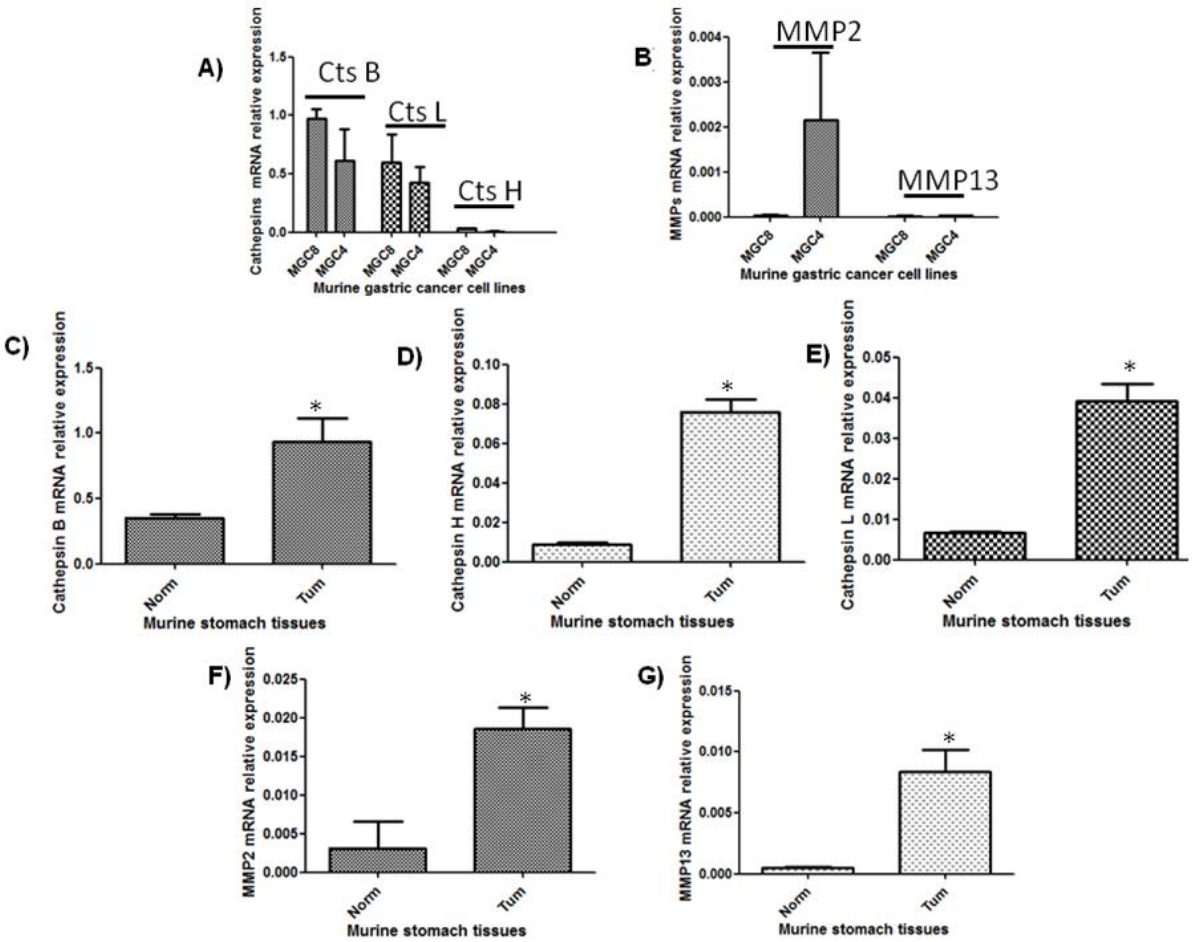

Figure 4-2: mRNA expression of cathepsin (Cts) and matrix metalloproteinases (MMPs) in murine gastric cancer cell lines and tissues. Murine gastric cancer cell lines were grown to exponential phase and total RNA was isolated, reverse transcribed and qPCR was carried out to determine the level of mRNA expression of cathepsins (Cts) **(A)** and matrix metaloprotinases (MMPs) **(B).** Cyclophilin was used as a house keeping gene. Data are presented as mean and standard error of the mean (S.E.M). mRNA expression of cathepsin (Cts) and matrix metalloproteinases (MMPs) in murine stomach tissues was determined **(C-G):** Stomach from *CEA-TAG* mice was opened and washed with PBS and total RNA was isolated. Reverse transcription and qPCR was performed to determine level of expression of Cts **(C-E**) and MMPs **(F-G)** in cancerous tissues and normal mucosa. Cyclophilin was used as a house keeping gene. At least three mice were included in the experiment. Experiments were done in triplicates and data are presented as mean and standard error of the mean (S.E.M). Student`s two tailed t-test: * $p<0.05$ (Tumor versus normal mucosa) *value* was considered as siginificant.

It is noteworthy to mention that the expression pattern of cathepsins in human gastric cancer cell lines correlated with that of murine ones. This was the reasons to investigate the expression patterns of relevant cathepsins and MMPs in a murine gastric cancer model. In this regard, RNA was extracted from cancerous and adjacent normal mucosa of *CEA-TAG* mice and qPCR was performed for both cathepsins and MMPs. As expected, elevated expression of cathepsins (B, H and L) and MMP2 was observed from cancerous tissues of stomach of *CEA-TAG* mice. Interestingly, only marginal expression was observed in the adjacent normal mucosa (Figure 4-2 C-G).

To validate the expression of cathepsins and to examine the specifity of the corresponding proteins to tumor tissues, immunohistochemistry was performed. In contrast to other cathepsins, stronger staining for cathepsin B was observed in tumor region of the stomach of *CEA-TAG* mice. Very weak siginal of all proteases was observed from the adjacent normal mucosa (Figure 4-3 A and B). This is in agreement with qPCR results described in Figure 4-2. Similarly, stronger stainings for cathepsins H and L, MMP2 and MMP3 were observed in tumor tissues than the adjacent normal mucosa (Figures 4-3 C-F).

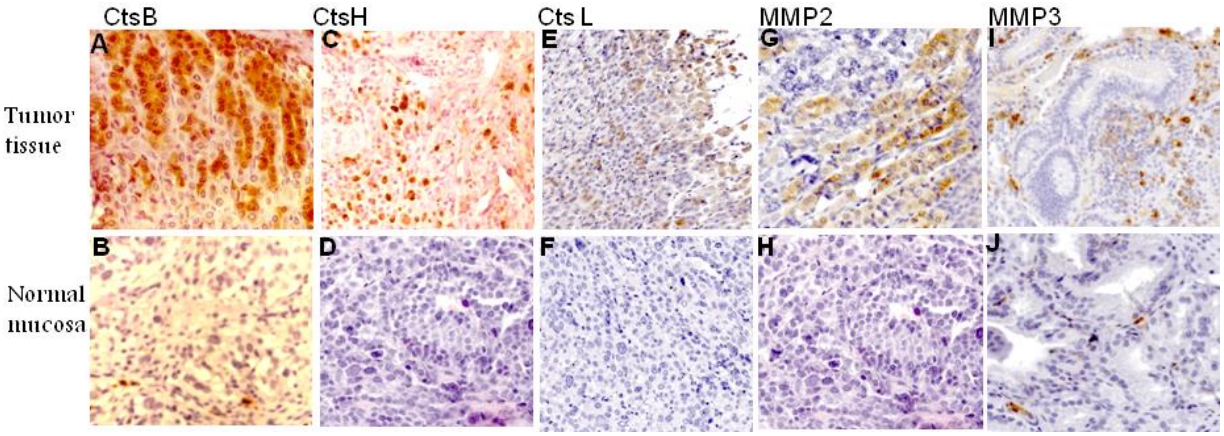

Figure 4-3: Immunohistochemistry of cathepsins (Cts) and matrix metalloprotinases (MMPs) in murine gastric cancer and normal adjacent mucosa. Stomach tissue from *CEA-TAG* mice was stained with antibodies specific for cathepsins B, H and L and matrix metalloprotinases MMP2 and MMP3. The upper row is from cancer tissues whereas the lower row is from adjacent normal mucosa.

In the same fashion, immunohistochemistry for representative MMPs was performed in murine stomach tissues. Higher expression of MMP2 and MMP3 was detected in cancerous tissues than the adjacent normal mucosa (Figure 4-3 G-J) whereas no significant expressions of other MMPs except MMP2 and 3 were detected in gastric cancer specimens.

4.1.2. Activation of the cathepsin-activable NIRF probe in gastric cancer

Cathepsins B, H, L, and S are activators of an established near infra red fluorescent (NIRF) probe that is based on fluorescence resonance energy transfer (Mohamed and Sloane, 2006). To investigate activation of the cathepsin-activable near infrared fluorescent (NIRF) probe (prosense-750) *in vivo*, 150µl of prosense-750 was intravenously (i.v) injected into *CEA-TAG* mice bearing gastric cancer. Twenty-four hours after intravenous adminstration of the probe, the mouse was sacrified, the stomach tissues were prepared and visualized on an Odyssey planar near-infrared scanner to detect the signal of the NIRF probe. Tissue sections displayed a strong signal (Figure 4-4 A and B) emitted by the cleavage of NIRF probe in stomach tumor.

Normal parts of stomach mucosa in fundus and corpus region displayed unspecific background autofluorescence, which was also observed in non-injected control mice (Figure 4-4 D and E). Immunohistochemical stainings for cathepsin B indicated that gastric tumors of both prosense-injected and the contol (non-injected) littermates displayed strong signal (Figure 4-4 C and F).

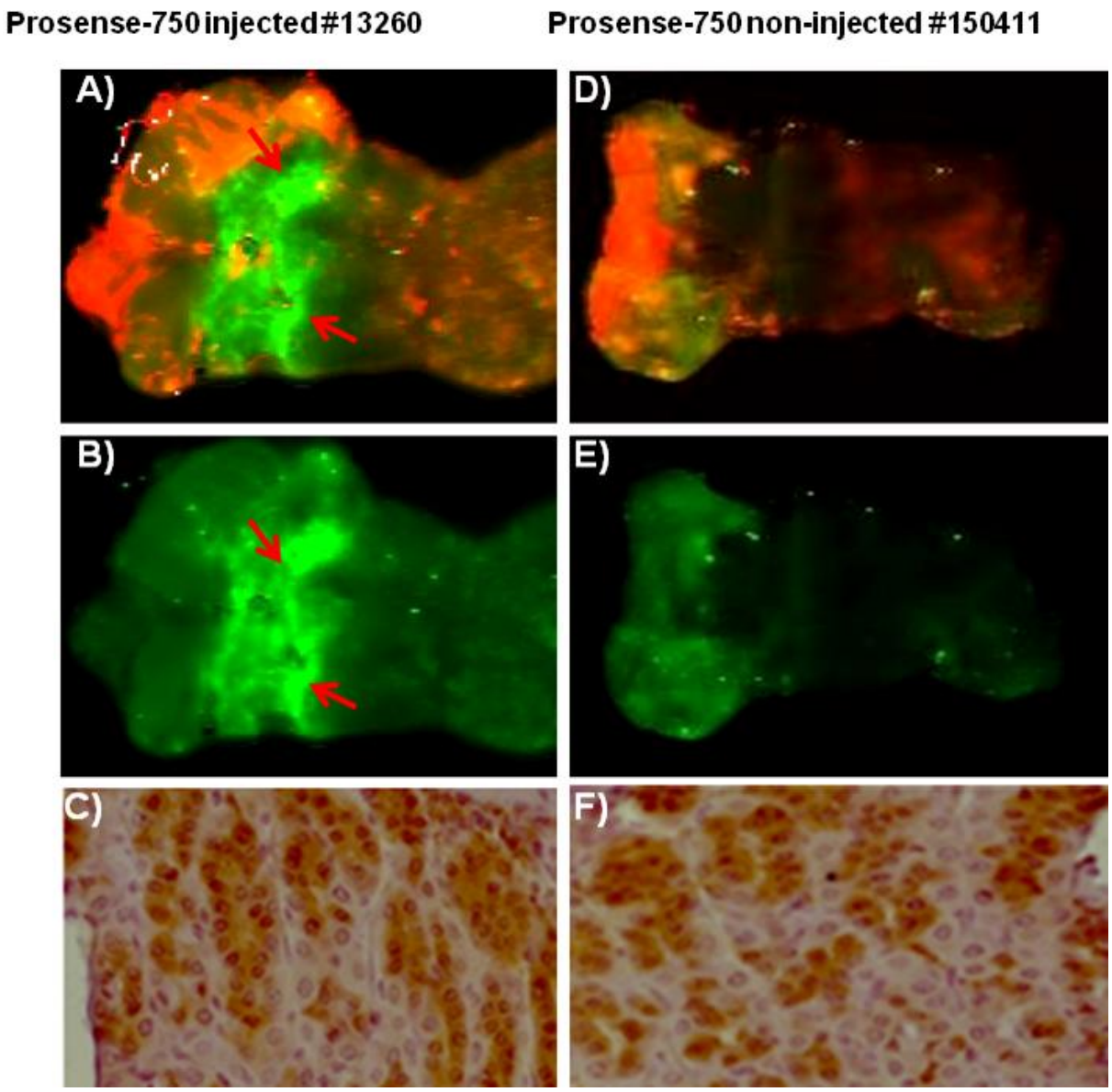

Figure 4-4: Cathepsins activate NIRF-activable probe. NIRF imaging of stomach tissues from *CEA-TAG* mice, bearing stomach tumor, indicates strong signal towards the antrum **(A and B)**. Mice not injected with the probe served as controls **(D and E)**. Tissues were harvested 24 h after i.v injection of the cathepsin-activatable NIRF probe. Stomach tissues were then scanned with a planar Odyssey near-infrared reader at 800 nm for visualization of the NIRF probe. The NIRF-probe signal is shown in green. Bright field imaging (red colour) to show the backgoround was performed at 680 nm. IHC analysis of probe-injected **(C)** and non-injected **(F)** mice indicates that cathepsins are expressed in both animals stomach tissues.

4.2. Treatment evaluation of gastric cancer

4.2.1. Response of gastric cancer cell lines to HDACis

Six human and 2 murine gastric cancer cell lines were treated with 3 different HDACis: SAHA (vorinostat), 4SC-201 and 4SC-202 and their corresponding IC_{50} values were determined. Dose dependent response against SAHA treatment was observed in all cell lines under investigation (Figure 4-5). The highest and lowest IC_{50} values for SAHA were detected in MKN45 and MGC8 cell lines, respectively (Table 4-1).

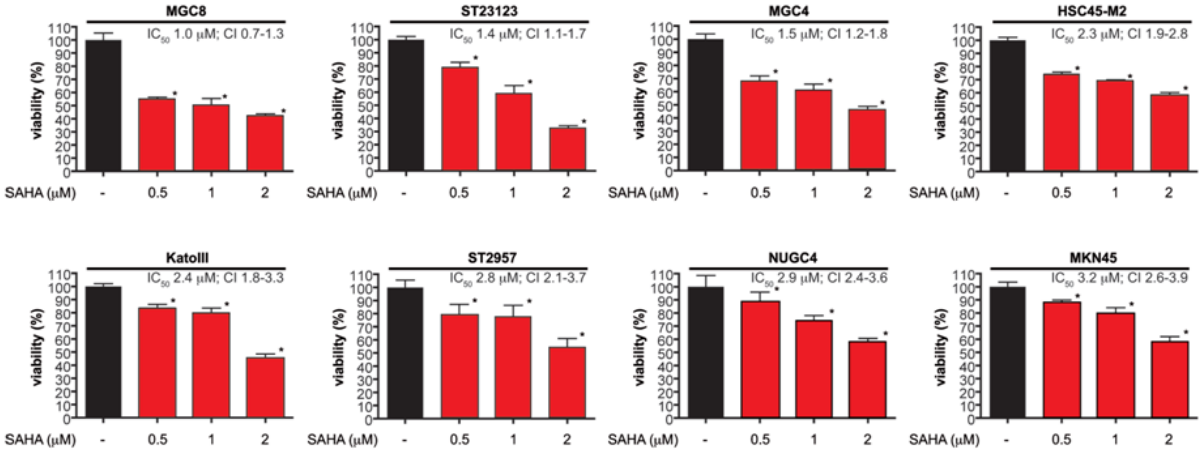

Figure 4-5: **Dose dependent response of gastric cancer cells to SAHA treatment**. Gastric cancer cell lines were treated with SAHA or were left as a vehicle treated control. A colorimetric MTT assay was performed to determine viability of the cells after 24 hours of treatment. IC_{50} values and the corresponding 95% confidence interval (CI) were depicted for each cell line. Three independent experiments were done in triplicates and data are presented as mean and standard error of the mean (S.E.M). (Student`s t-test: * $p<0.05$ versus controls).

Table 4-1: Response of gastric cancer cell lines against SAHA treatment.

Cell line	SAHA IC50 (48 hrs) (µM SAHA)	SAHA CI (95%)
MGC8	1.0	0.7-1.3
ST23132	1.4	1.1-1.7
MGC4	1.5	1.2-1.8
HSC45-M2	2.3	1.9-2.8
KatoIII	2.4	1.8-3.3
ST2957	2.8	2.1-3.7
NUGC4	2.9	2.4-3.6
MKN45	3.2	2.6-3.9

Besides, Hoechst staining was performed for relatively sensitive and non-responding cell lines for SAHA treatment and apoptotic fractions were determined. As expected, it was determined that the nonresponding cell line (MKN45) against SAHA treatment displayed lower apoptotic fractions whereas the vice versa was observed in sensitive cell line (MGC8) (Figure 4-6). Taken together, dose dependent reduction in viability and observation of higher apoptotic fractions in sensitive cell line indicated the importance of further investigation to determine how SAHA acts on these cell lines.

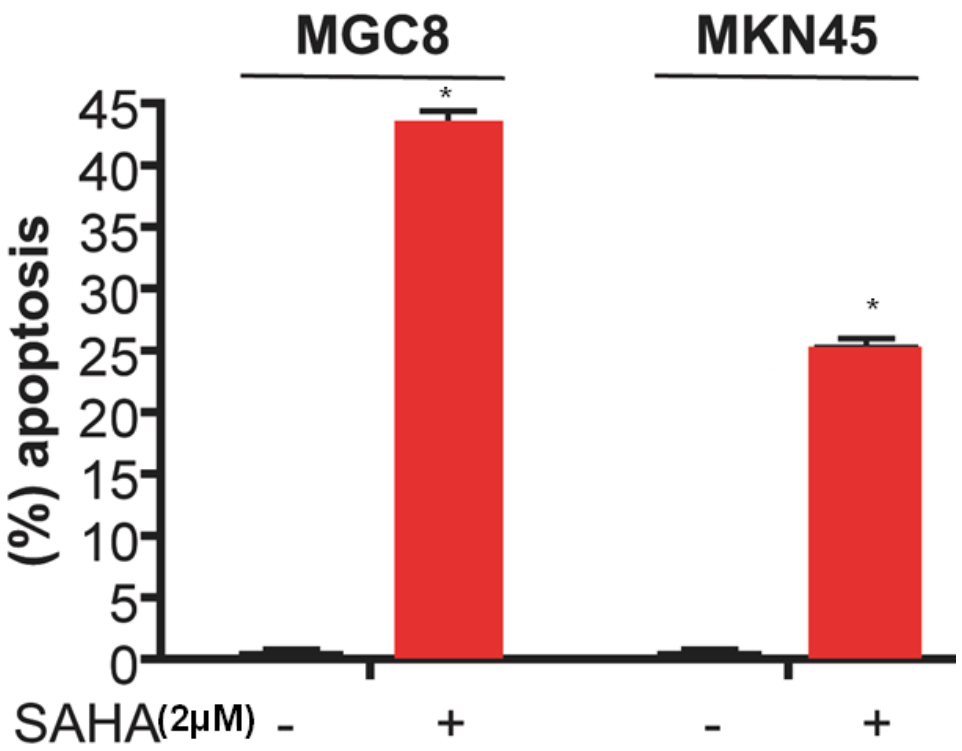

Figure 4-6: SAHA induces apoptosis in gastric cancer cell lines. MKN45 and MGC8 (human and murine, respectively) cell lines were treated with SAHA as indicated or were left as a vehicle treated control. After 12 hours of SAHA treatment apoptotic fractions were determined with Hoechst staining with the aid of inverted microscope equipped with UV. Three independent experiments were done in triplicates and data are presented as mean and standard error of the mean (S.E.M). (Student`s t-test: *p<0.05 versus controls).

Similarly, gastric cancer cell lines were treated with different concentrations of 4SC-201 and 4SC-202. Dose dependent reduction in viability was detected (Figure 4-7A and B) and the IC_{50} values of 4SC-202 (Table4-2) indicated that MGC8 (IC_{50}=6.6) is relatively the most nonresponding whereas ST2957 (IC_{50}=0.6) cell line is the most sensitive (Figure 4-7B). In contrast, MGC8 (IC_{50}=1.2) is relatively the most susceptible for 4SC-201 whereas ST2957 (IC_{50}= 3.7) is among the top nonresponding cell lines (Figure 4-7A).

Table 4-2: Response of gastric cells lines to 4SC-201 and 4SC-202.

Cell line	IC50 (48 hrs) (µM4SC-201)	4SC-201 (95% CI)	Cell line	IC50(48 hrs) (µM 4SC-202)	4SC-202 (95% CI)
MGC8	1.2	0.5-0.7	ST2957	0.6	0.7-1.1
MGC4	1.6	0.3-0.4	HSC45-M2	1.0	0.4-0.5
ST23132	1.8	0.4-0.9	MKN45	1.1	0.8-1.1
HSC45-M2	2.7	0.4-0.4	ST23132	1.2	0.4-0.5
MKN45	3.3	0.4-0.8	KatoIII	1.3	0.9-1.1
NUGC4	3.4	0.1-0.8	MGC4	2.0	0.1-0.2
ST2957	3.7	0.1-0.4	NUGC4	3.0	0.1-0.3
KatoIII	4.3	0.1-0.2	MGC8	6.6	0.1-0.2

The fact that MGC8 is the most sensitive to both SAHA and 4SC-201 whereas ST2957 is among the top nonresponding groups might indicate that these HDACis might have a common mechanism to act on the cellular machinaries. However, the underlying molecular mechanisms how the 4SC-201 and 4SC-202 act on the cellular physiology is entirely unknown and beyond this study.

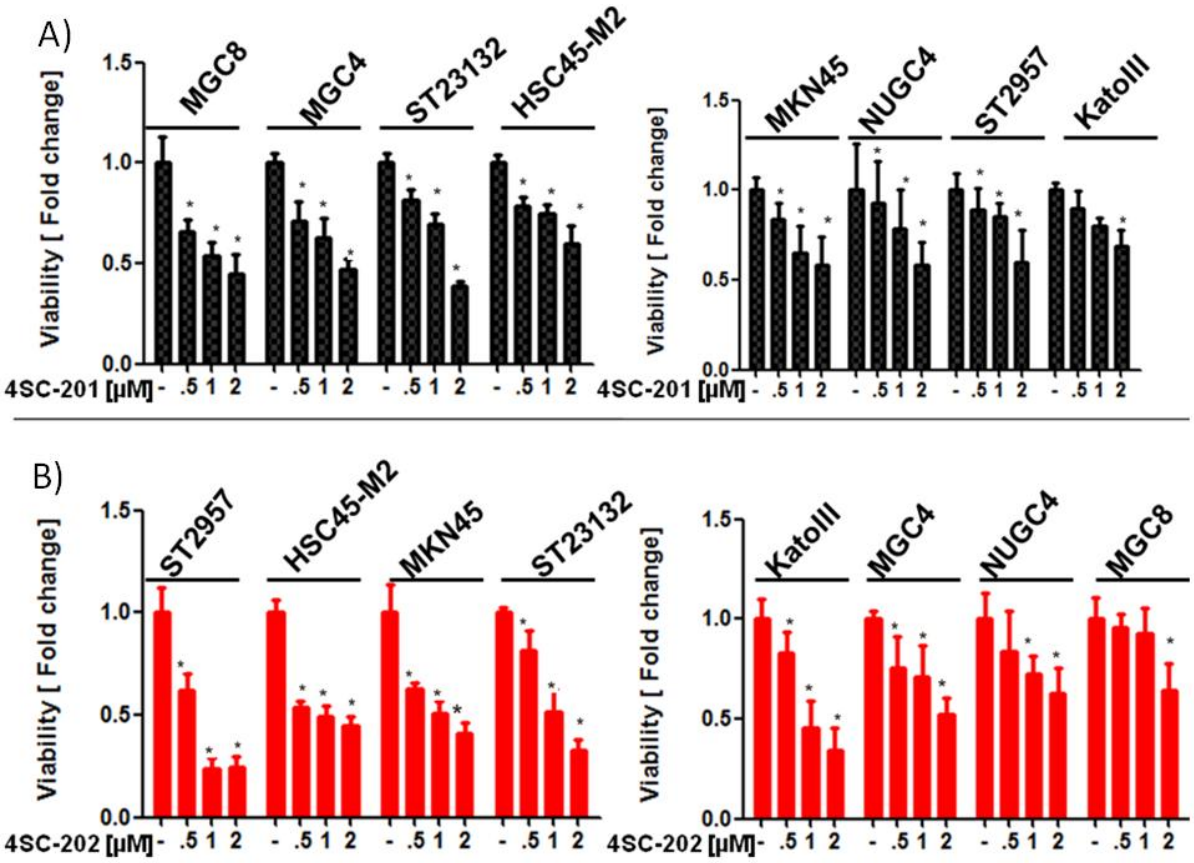

Figure 4-7: Dose dependent response of gastric cancer cell lines to 4SC-201 and 4SC-202 treatment. Gastric cancer cell lines were treated with 4SC-201 **(A)** and 4SC-202 **(B)** or were left as a vehicle treated control. A colorimetric MTT assay was performed to determine viability of the cells after 24 hours of treatment. Three independent experiments were done in

triplicates and data are presented as mean and standard error of the mean (S.E.M). (Student`s t-test: * $p<0.05$ versus controls).

4.2.2. BCL_{XL} and MCL1 expression levels inversely correlate with the responsiveness of gastric cancer cells towards HDACi

To elucidate the reason why SAHA was not so potent to reduce viability of gastric cancer cell lines efficiently, the endogenous expression level of antiapoptotic proteins was determined by western blot. As shown in Figure 4-8 A, the highest BCL_{XL} and MCL1 expression was observed in cell lines with highest SAHA IC_{50} value. Thus, the expression pattern of both BCL_{XL} and MCL1 was correlated with SAHA IC_{50} values and a first hint that both proteins modulate the response of gastric cancer cells to HDACi was drawn from this correlation.

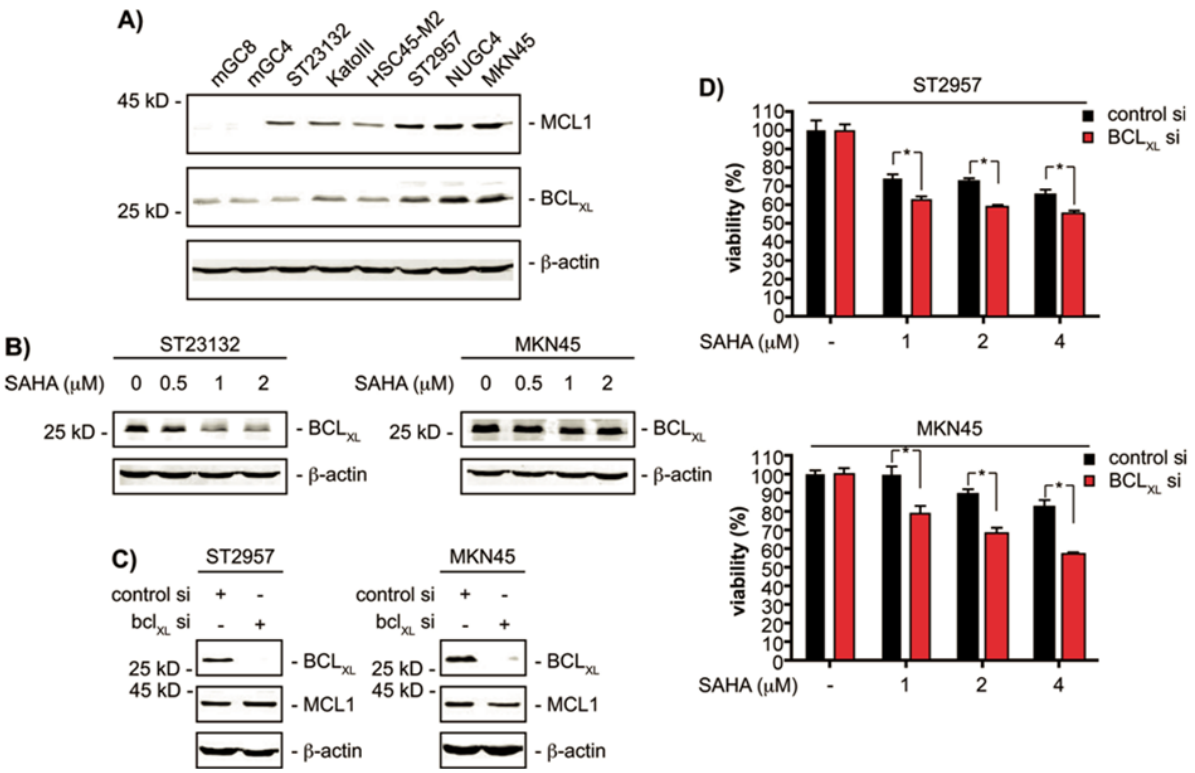

Figure 4-8: BCL_{XL} restricts SAHA efficacy of gastric cancer cells. **A)** Western blot analysis of MCL1 and BCL_{XL} expression of the indicated gastric cancer cell lines. β-actin was used as loading control. **B)** ST23132 and MKN45 cells were treated with increasing doses of SAHA for 24 hours as indicated or were left as vehicle treated controls. Expression of BCL_{XL} was detected by western blot and β-actin served as loading control. **C)** ST2957 and MKN45 cells were transfected with the indicated siRNAs. Fourty eight hours after the transfection, whole-cell lysate was prepared and expression of BCL_{XL}, MCL1 were detected by western blots and β-actin was used as loading control. **D)** ST2957 and MKN45 were transfected with the indicated siRNAs. Fourty eight hours after the transfection, cells were treated with SAHA as indicated for additional 24 hours. Viability of cells was measured in MTT assays. Three independent experiments were done in triplicates and data are presented as mean and standard error of the mean (S.E.M). (Student`s t-test: * $p<0.05$ versus controls).

4.2.3. BCL_{XL} and MCL1 counteract efficacy of HDACi

To investigate regulation of BCL_{XL} by HDACi, cells were treated with SAHA and a series of western blot analysis were performed. BCL_{XL} protein expression was reduced slightly in the SAHA sensitive ST23132 cell lines (IC_{50} 1.4 µM) whereas no regulation of BCL_{XL} was detected in the more resistant MKN45 cells (IC_{50} 3.2 µM) (Figure 4-8B). Hence, downregulation of BCL_{XL} might characterize gastric cancer cells with low SAHA IC_{50} values. Further to confirm this result, RNAi was used to analyze the contribution of BCL_{XL} for cellular responses towards SAHA. Knockdown of this protein in ST2957 (IC_{50} 2.8 µM) and MKN45 cells were specific and did not have any impact on MCL1 expression level (Figure 4-8C). In both cell lines, a reduction of BCL_{XL} decreased the viability of both cell lines upon treatment with SAHA (Figure 4-8D). Thus, BCL_{XL} limits the pro-apoptotic potency of SAHA against gastric cancer cells. It has been also reported that SAHA induced apoptosis is restrained by high expression of BCL_{XL} and BCL2 proteins (Vrana *et al*., 1999). Likewise, HADCis induce apoptosis in leukemic cells without decreasing the level of MCL1 protein expression (Inoue *et al*., 2008).

SAHA treatment altered MCL1 expression neither in ST23132 nor in MKN45 gastric cancer cell lines (Figure 4-9A). This is in consistant with recent observation that attenuation of MCL1 levels was reported to enhance HDACi-induced cytotoxicity in leukemic cells (Inoue *et al*., 2008). Thus, it was important to test how MCL1 affects the HDACi responses of the cellular systems under investigation. To this end, both ST2957 and MKN45 cell lines were transiently transfected with siRNA specific to *MCL1*. Knockdown of *MCL1* with RNAi in these cell lines was specific and did not influence BCL_{XL} expression (Figure 4-9B). The reduction of MCL1 protein expression slightly increased the SAHA induced therapeutic response of ST2957 and MKN45 cells (Figure 4-9C). The fact that this observation reached statistical significance argues that MCL1 counteracts HDACi-induced death programs in gastric cancer cells.

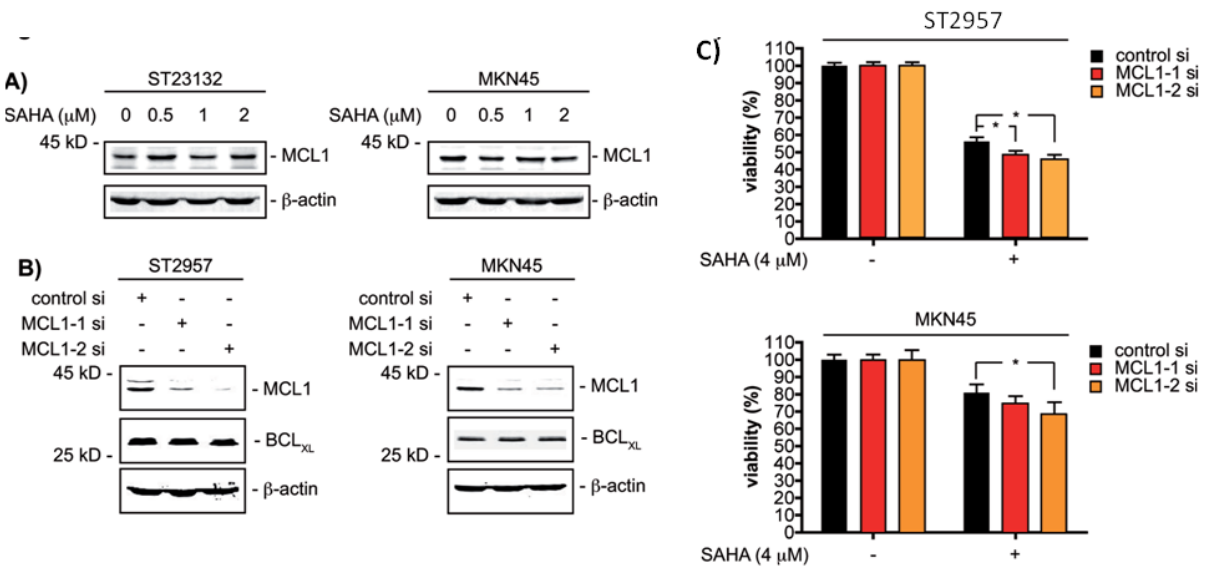

Figure 4-9: MCL1 restricts SAHA efficacy of gastric cancer cells. A) ST23132 and MKN45 cells were treated for 24 hours with increasing doses of SAHA as indicated or left as vehicle treated controls. Western blots detected expression of MCL1 and β-actin (loading control). **B)** ST2957 and MKN45 cells were transfected with the indicated siRNAs. Fourty eight hours after transfection whole-cell lysates were prepared and western blots detected expression of MCL1, BCL_{XL} and β -actin (loading control). **C)** ST2957 and MKN45 cells were transfected with the indicated siRNAs. Fourty eight hours after the transfection, cells were treated with SAHA as indicated for additional 24 hours. Viability of cells was measured in MTT assays. Three independent experiments were done in triplicates and data are presented as mean and standard error of the mean (S.E.M). (Student`s t-test: * $p<0.05$ versus controls).

4.2.4. c-MYC controls BCL_{XL}, MCL1 and the HDACi response

Given that MCL1 and BCL_{XL} counteract the HDACi response, the pathways involved in controlling their expression in gastric cancer cell lines were deciphered. First, NFκB and STAT3 pathways were investigated since they were linked to the therapeutic resistance of other cancer cells towards HDACi (Spange *et al*., 2009). However, no correlation between the IC_{50} values of gastric cancer cell lines and NFκB/RelA expression was observed (Figure 4-10A). Furthermore, knockdown of this transcription factor did not change expression of MCL1 and BCL_{XL} (Figure 4-10B). Similarly, knockdown of STAT3 did not change the expression of MCL1 and BCL_{XL} (Figure 4-10C).

It has been indicated that c-MYC overexpression was detected in over 45% of the gastric cancer cases and it is associated with a poor clinical course of gastric cancer in both intestinal and diffuse-types of gastric adenocarcinoma (Zhang *et al.*, 2010). In addition, since the expression pattern of genes regulated by c-MYC are linked with

therapeutic resistance (Mizutani *et al*., 1994; Leonetti *et al*., 1999; Sklar and Prochownik, 1991), c-MYC was considered as a factor determining the fate of cells treated with HDACi. Thus, western blot was performed to observe the expression pattern of c-MYC, its role in regulating pro-survival proteins (BCL_{XL} and MCL1) and its link with the response of gastric cancer cell lines towards HDACi. Interestingly, knockdown of c-MYC resulted in a marked reduction in protein and mRNA expression of MCL1 in ST2957 and MKN45 gastric cancer cells (Figure 4-10 D and E).

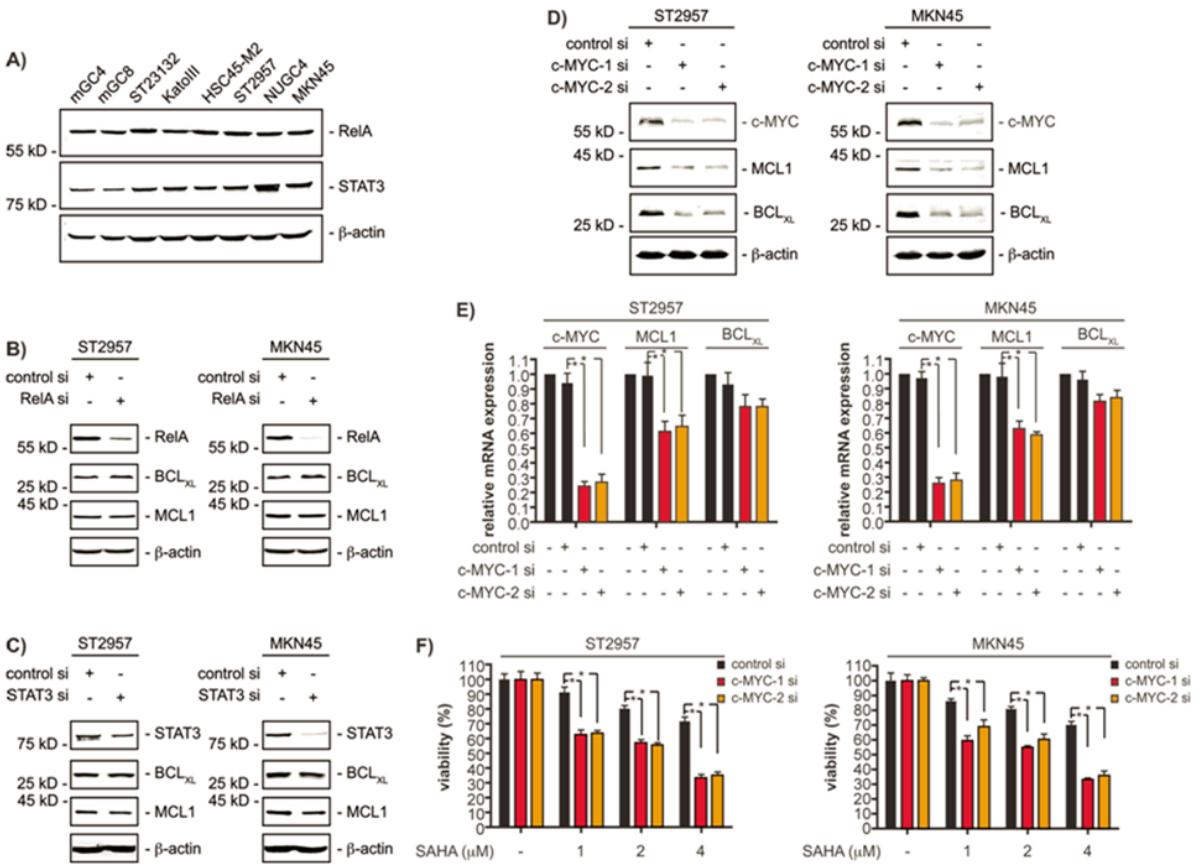

Figure 4-10: c-MYC controls MCL1 and BCL_{XL} expression of gastric cancer cells. A) Western blots of whole cell lysates of the indicated gastric cancer cell lines detected expression of STAT3, RelA and β-actin (loading control). **B)** and **C)** ST2957 and MKN45 cells were transfected with the indicated siRNAs. Fourty eight hours after the transfection whole-cell lysates were prepared and western blots detected expression of RelA (**B)**, STAT3 (**C)**), BCL_{XL}, MCL1 and β-actin (loading control). **D)** ST2957 and MKN45 cells were transfected with the indicated siRNAs. Fourty eight hours after the transfection whole-cell lysates were prepared and western blots detected expression of c-MYC, BCL_{XL}, MCL1 and β-actin (loading control). **E)** ST2957 and MKN45 cells were transfected with the indicated siRNAs. Fourty eight hours after the expression of *c-MYC, MCL1* and *BCL_{XL}* mRNAs were determined by qPCR using cyclophilin A mRNA as reference. **F)** ST2957 and MKN45 cells were transfected with the indicated siRNAs. Fourty eight hours after the transfection cells were treated with SAHA as indicated for additional 24 hours. Viability of cells was measured in MTT assays. Three independent experiments were done in triplicates and data are presented as mean and standard error of the mean (S.E.M). (Student`s t-test: * $p<0.05$ versus controls).

Whereas the expression level of BCL_{XL} protein was distinctly reduced in *c-MYC* knockdown cells (Figure 4-10D), the reduction in BCL_{XL} mRNA expression level was not significant (Figure 4-10E). This was the first hint that indicated c-MYC as a potential upstream regulator of BCL_{XL} and MCL1 in gastric cancer cells. Furthermore, these observations lead to the question how c-MYC regulates BCL_{XL} at a non-genomic level. To investigate the effect of knockdown of c-MYC on HDACi-nonresponding cell lines, cells were transiently transfected with siRNA specific to *c-MYC* and viability assay was carried out. As shown in figure 4-11, transfection of cells with siRNA specific to *c-MYC* resulted in significantly reduced viability and the potential of SAHA to induce apoptosis was augmented by treating cells with myc-I and SAHA in combination (Figure 4-12).

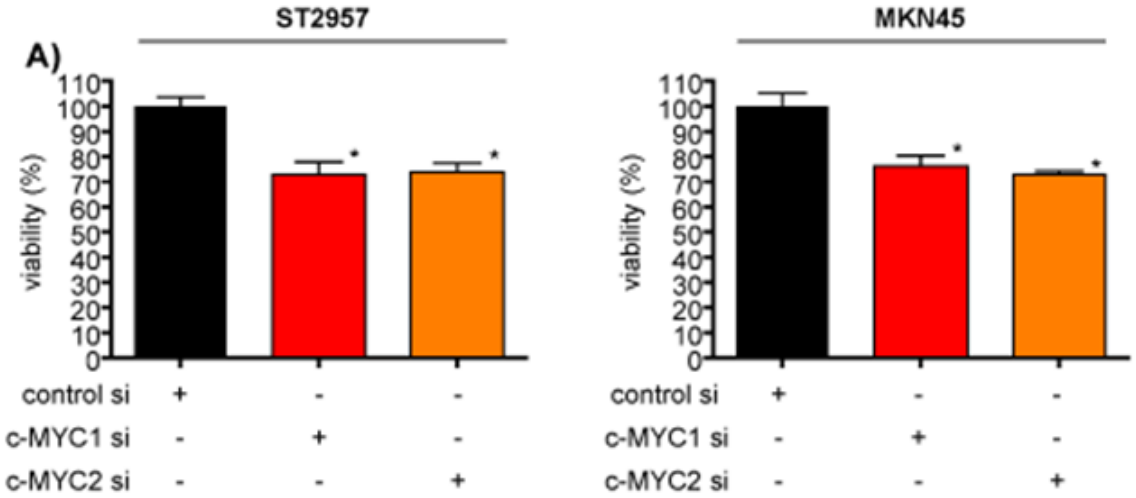

Figure 4-11: *c-MYC* knockdown reduces viability of gastric cancer cell lines. ST2957 and MKN45 cell lines were transfected with the indicated siRNAs. Fourty eight hours after the transfection viability of cells was measured in MTT assays. Three independent experiments were done in triplicates and data are presented as mean and standard error of the mean (S.E.M). (Student`s t-test: * $p<0.05$ versus controls).

Moreover, knock down of *c-MYC* in relatively resistant gastric cancer cell lines (ST2957 and MKN45) enhanced the cellular response towards SAHA treatment (Figure 4-10F). This indicates that the transcriptional factor c-MYC appears to counteract the effects of HDACi on gastric cancer cells. To validate the results obtained by RNAi experiments, ST2957 and MKN45 cells were treated with the c-MYC inhibitor (myc-I), which functions by interfering with the heterodimerization of c-MYC/MAX (Yin *et al*., 2003). As a result, dose-dependent downregulation of MCL1 and BCL_{XL} was observed in both cell lines after pharmacological inhibition of c-MYC

(Figure 4-13A). It was interesting to investigate how c-MYC was regulating these two important prosurvival factors. To this end, quantitative Chromatin Immunoprecipitation (qChIP) was performed to test if c-MYC binds directly to the *MCL1* promoter region. Interestingly, it was observed that c-MYC was recruited to the promoter region of the *MCL1* gene in MKN45 as well as ST2957 cell lines. As expected, binding of c-MYC was reduced after treatment of both cell lines with the myc-I (Figure 4-13B). Furthermore, c-MYC enrichment at promoter region of MCL1 was correlated with the recruitment of RNA polymerase II to the *MCL1* promoter, indicating that MCL1 mRNA is actively transcribed under the control of c-MYC in untreated cell lines. The recruitment of RNA PolI to *MCL1* promoter is signifiantly reduced after treatment of cells with myc-I (Figure 4-13C).

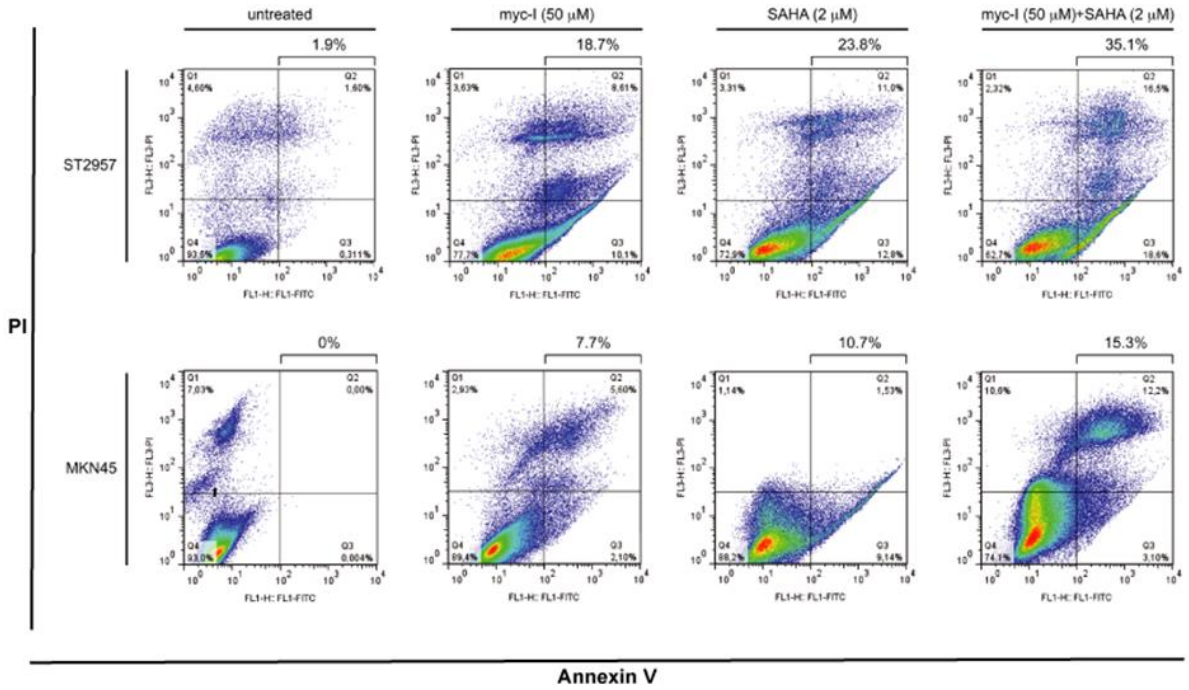

Figure 4-12: c-MYC induces apoptosis in gastric cancer cells. ST2957 and MKN45 cells were treated with the MYC inhibitor (myc-I, 10058-F4), SAHA, the myc-I and SAHA for 24 hours or were left as an untreated control. Cells were stained with propidium iodide (PI) and FITC labeled anti-Annexin V. Depicted is the Annexin V positive fraction (early apoptosis=Annexin V+/PI- and late apoptosis= Annexin V+/PI+). (Student`s t-test: * $p<0.05$ versus controls).

In agreement with the role of c-MYC as survival factors for gastric cancer cell lines, treatment of cells with myc-I significantly increased the response of cells to SAHA (Figure 4-13D). In addition, transfection of cells with siRNA specific to *c-MYC* significantly augmented the SAHA response in ST2957 and MKN45 cells (Figure 4-10F). The potential of apoptosis induction of SAHA was further increased by co-

treatment of the cell lines with myc-I (Figure 4-13E). Taken together, these data confirm a role for c-MYC in tumor maintenance of gastric cancer cells (Chen *et al*., 2001; Khanna *et al*., 2009) and also indicate c-MYC as a therapeutic target in gastric cancer.

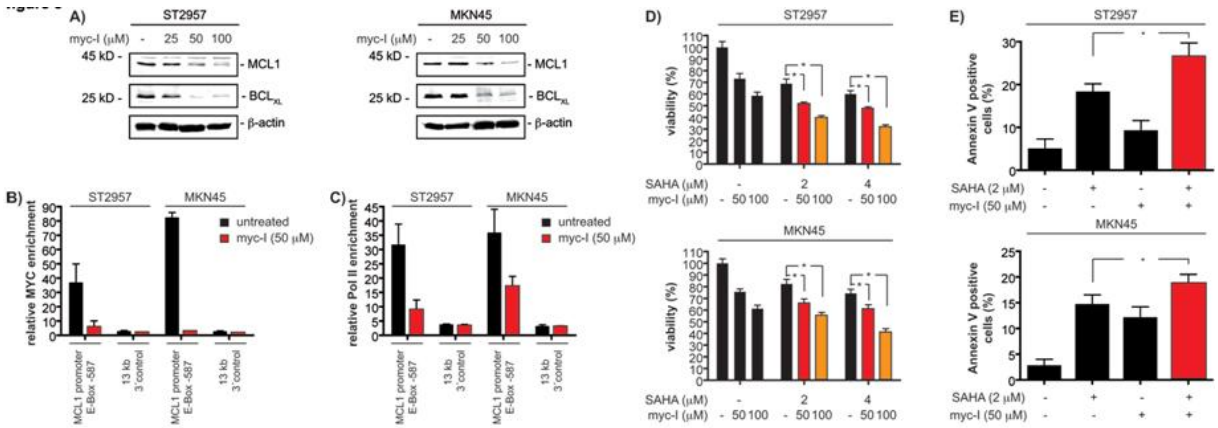

Figure 4-13: *MCL1* is a direct c-MYC target in gastric cancer cells. A) ST2957 and MKN45 cells were treated with the myc-I for 24 hours. Western blots detected the expression of BCL_{XL}, MCL1 and β-actin (loading control). **B)** and **C)** ST2957 and MKN45 cells were treated with the myc-I for 24 hours or were left as a vehicle treated control. ChIP analysis revealing the binding of c-MYC (**B)**) or the RNA Polymerase II (**C)**) to the E-box of the *MCL1* promoter or a 13 kb 3` control. **D)** ST2957 and MKN45 cells were treated with the myc-I, SAHA, the myc-I and SAHA for 24 hours or were left as an untreated control. Viability of cells was measured using MTT assays. Three independent experiments were done in triplicates and data are presented as mean and standard error of the mean (S.E.M). (Student`s t-test: * p<0.05 versus controls). **E)** ST2957 and MKN45 cells were treated with the myc-I, SAHA and the combination of both for 24 hours as indicated or were left as an untreated control. Cells were stained with Propidium iodide (PI) and FITC labeled anti-Annexin V. Depicted is the Annexin V positive fraction (early apoptosis=Annexin V+/PI- and late apoptosis= Annexin V+/PI+). (Student`s t-test: * *p*<0.05 versus controls).

4.2.5. c-MYC-induced transcription of *eIF4E* regulates BCL_{XL} expression in gastric cancer cells

The *c-MYC* oncogene is an important transcriptional factor that regulates a variety of genes related to proliferation, differentiation, and apoptosis (Meyer and Penn, 2008). It has been also observed that c-MYC regulates protein translation, e.g. through control of genes coding for translation initiation factors, such as *eIF4E* (Lin *et al*., 2008; Jones *et al*., 1996; Pelengaris *et al*., 2002; Rosenwald *et al*., 1993). Accordingly, downregulation of *eIF4E* expression was observed in c-MYC siRNA transfected ST2957 and MKN45 cells at protein (Figure 4-14A) and mRNA levels (Figure 4-14B). Furthermore, myc-I treated gastric cancer cell lines also displayed remarkably reduced eIF4E expression (Figure 4-14C).Therefore, it was important to know how c-MYC is regulating *eIF4E* in gastric cancer cell lines under investigation.

To proof direct transcriptional regulation of *eIF4E* by c-MYC, qChIP assay was performed. In similar fashion as the *MCL1* promoter, the recruitment of c-MYC to the E-box in the proximal *eIF4E* promoter was observed. As expected, recruitment of this transcription factor to *eIF4E* promoter was hampered after treatment of cells with myc-I (Figure 4-14D). Moreover, reduced recruitment of c-MYC to the *eIF4E* promoter region was accompanied by a decrease in binding of RNA polymerase II to *eIF4E* promoter in ST2957 and MKN45 cells (Figure 4-14E). Taken together, these findings indicate that c-MYC is regulating *eIF4E* in gastric cancer cells, directly by binding its promoter region

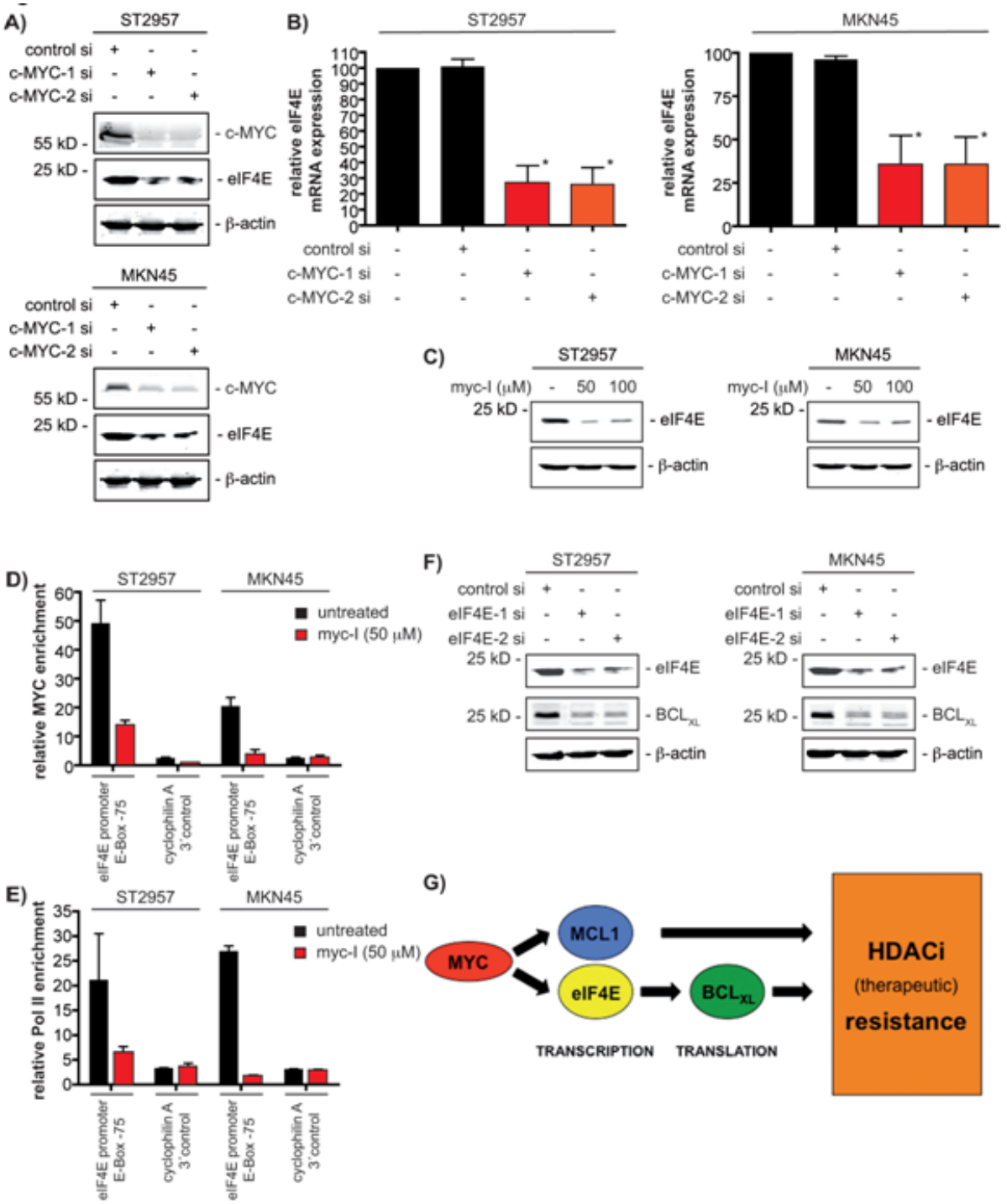

Figure 4-14: c-MYC controls *eIF4E* transcription to regulate BCL$_{XL}$ expression in gastric cancer cells. A) ST2957 and MKN45 cells were transfected with the indicated siRNAs. Fourty eight hours after the transfection whole-cell lysates were prepared and western blots detected expression of c-MYC, eIF4E and β-actin (loading control). **B)** ST2957 and MKN45 cells were transfected with the indicated siRNAs. Fourty eight hours after the expression of the *eIF4E* mRNA were determined by qPCR using cyclophilinA mRNA as reference. **C)** ST2957 and MKN45 cells were treated with the myc-I for 24 hours. Western blots detected the expression of eIF4E and β-actin (loading control). **D)** and **E)** ST2957 and MKN45 cells were treated with the myc-I for 24 hours or were left as a vehicle treated control. ChIP analysis revealing the binding of c-MYC **(D)** or the RNA Polymerase II **(E)** to the E-box of the *eIF4E* promoter or a cyclophilin A 3`control. **F)** ST2957 and MKN45 cells were transfected with the indicated siRNAs. Fourty eight hours after the transfection whole-

cell lysates were prepared and western blots detected expression of eIF4E, BCL_{XL} and β-actin (loading control). **G)** Schematic presentation of how gene expression signatures induced by c-MYC restrain the efficacy of HDACi against gastric cancer cells. Three independent experiments were done in triplicates and data are presented as mean and standard error of the mean (S.E.M). (Student`s t-test: * $p<0.05$ versus controls).

Apart from regulation of BCL_{XL} by c-MYC at protein level, it was interesting to know the underlying mechanisms how c-MYC is regulating BCL_{XL} at genomic level. To this end, it was hypothesized that c-MYC might control BCL_{XL} via the translational initiation factor. To confirm regulation of BCL_{XL} expression by *eIF4E*, ST2957 and MKN45 cell lines were transiently transfected with siRNAs specific to *eIF4E*. The result indicated that transfection of ST2957 and MKN45 cells with such siRNAs clearly blocked BCL_{XL} expression at protein and mRNA level (Figure 4-14F). This is an important evidence that *eIF4E* is actively involved in promoting translations of proteins associated with survival of cancer cell lines. From these observations, it is possible to say that the translation of BCL_{XL} in gastric cancer cell lines was regulated by c-MYC-*eIF4E* axis.

5. Discussion

5.1. Early detection of gastric cancer

Currently high grade dysplasia and early gastric cancer are often missed during conventional endoscopic examination of the upper gastrointestinal tract (UGIT) (Enns, 2010; Leodolter *et al*., 2006; Telford and Enns, 2010). Candidate biomarker molecules that can be visualized by specific probes, labelled with fluorophores, are extremely needed to indicate high grade dysplasia and onset of early gastric cancer in endoscopic imaging. The pattern of expression of such biomarker molecules in normal tissues, early tumor and late metastasis varies according to their respective functions in cells. Some of such well studied cellular molecules are involved in angiogenesis, extracellular matrix degradation and dissemination of tumor cells (Keppler, 1996; Kuester *et al*., 2008; Mohamed and Sloane, 2006). Among potentially important factors for imaging early onset of gastric cancer are cathepsin proteases and matrix metalloprotinases (MMPs). Cathepsins are lysosomal cysteine proteolytic enzymes involved in several cellular functions including protein turnover, proliferation, invasion and metastasis whereas matrix metalloprotinases (MMPs) are zinc-dependent endopeptidases that are engaged in large variety of cellular physiology and pathology including tissue remodeling and metastasis (Gocheva and Joyce, 2007). They are frequently upregualted in cancer and other cancer associated cells. Cathepsins and MMPs have been reported to be promising tools for early detection of tumors in various organs (Bremer *et al*., 2001; Eser *et al*., 2011; Herszényi *et al*., 2008; Weissleder and Ntziachristos, 2003). In this study, the expression pattern of cathepsins and MMPs was determined in human and murine gastric cancer cell lines. In addition, the expression level of these enzymes in tumor and adjacent normal mucosa of murine stomach was evaluated. Cathepsins B, H and MMP2 were well expressed in human and murine gastric cancer cell lines and the corresponding murine stomach tumour tissues. This is consistent with findings in other tumour types (Eser *et al*., 2011; Herszényi *et al*., 2008; von Burstin *et al*., 2008). Illustrating critical importance of the application of proteases in the diagnosis of curable precursor lesions and early-stage cancer, Eser and his colleagues were able to differentiate between normal pancreatic tissue and low-grade pancreatic intraepithelial neoplasia (mPanINs), high grade mPanINs and early-stage pancreatic ductal adenocarcinoma (PDAC). Furthermore, immunohistochemistry with antibodies

specific to cathepsins and MMPs indicated that cathepsins B and H and MMP2 and MMP3 were more expressed in the *CEA-TAG* mice stomach tumor than adjacent normal mucosa. Taken together, these findings indicate that proteases are potentially involved in gastric carcinogenesis and could be potential biomarkers for early onset of gastric cancer in mouse models. Thus, these enzymes represent an attractive target for tumor imaging and therapeutic strategies. Moreover, these findings might point out that *CEA-TAG* mice serve as good mouse model for early gastric cancer detection and open an opportunity for monitoring and treatment evaluation of gastric cancer.

Since cathepsins B and H and MMP2 are highly expressed in gastric cancer, a cathepain activatable probe was used to test a proof of principle for feasibility to detect gastric cancer by fluorescent imaging. The probe was injected intravenously and 24 h later we performed *ex vivo* fluorescent imaging. We were able to show that gastric tumours show a stronger signal than adjacent normal mucosa. Therefore, imaging of cathepsin activity seems to be a promising strategy for gastric cancer detection by endoscopic fluorescent imaging of the stomach. However, further studies are neccessary to answer the following questions:

1. Is it possible to detect precancerous gastric lesions and early gastric cancer by imaging of protease activity *in vivo*?

2. Are cathepsin B and H or MMP2 involved in gastric carcinogenesis and progression and do they predict prognosis in gastric cancer patients?

3. Is it possible to monitor therapeutic response by imaging of cathepsin B and H or MMP2?

Furthermore, cathepsin B and H or MMP2 proteases are perhaps important molecules to mark the boundary between normal tissue and tumorigenic tissue, enhancing the efficacy of gastric cancer surgery.

5.2. Treatment evaluation of gastric cancer

The application of multimodal treatment protocols that rely mainly on cisplatin and 5 fluorouracil (5-FU) did not improve the outcome of advanced gastric carcinoma patients (Mutze *et al*., 2010). However, systemic chemotherapy still remains one of the key treatment options for patients with advanced gastric cancer. Compared to best supportive care, chemotherapy in advanced gastric cancer improves median survival (Wagner *et al*., 2005). Neverthless, it is palliative and 5-year survival rates are below 20%. Histone deacetylase inhibitors (HDACis) are currently tested in advanced gastric cancer, but the molecular mechanisms and markers relevant for the efficacy of HDACis in gastric cancer treatment are largely equivocal (Tabernero *et al.,* 2005). In this study, the role of three HDACis namely SAHA, 4SC-201 and 4SC-202 in gastric cancer treatment was investigated. Dose dependent response of gastric cancer cell lines towards HDACis was observed. Treatment of gastric cancer cells with 4SC-201 and 4SC-202 resulted in marked decrease in viability. The similarity in the pattern of IC_{50} values of SAHA and 4SC-201 in sensitive and nonresponding cell lines indicate that these HDACis might have a common mechanism to act on the cellular machinaries. However, the underlying molecular mechanisms how the 4SC-201 and 4SC-202 act on the cellular physiology is entirely unknown and beyond this study. Therefore, this study investigated the molecular mechanisms that hamper efficacy of SAHA as a potential HDACi for gastric cancer treatment.

Here, it is revealed that c-MYC counteracts SAHA efficacy in gastric cancer cells by regulating the expression of the prosurvival BCL2 family members, BCL_{XL} and MCL1. These findings demonstrate two independent mechanisms by which c-MYC protects gastric cancer cell lines from HDACi. Firstly, c-MYC directly controls transcription of *MCL1 by* binding its promoter region. Secondly, regulation of BCL_{XL} protein expression was attributed to c-MYCs´ capability to control the *eIF4E* gene and thereby translation of the BCL_{XL} mRNA (Figure 4-14G). One of the fundamental responses of cells treated with HDACi is programmed cell death-apoptosis (Frew *et al*., 2009). Induction of apoptosis in cancer cells by such inhibitors predicts a beneficial therapeutic success of these agents (Lindemann *et al*., 2007). Consistently, it is observed that the pro-survival BCL2 family members BCL_{XL} and MCL1 limit the efficacy of HDACi in a cell-based model of gastric cancer cells. Furthermore, these results are in line with *in vivo* and *in vitro* results that demonstrated that the efficacy of HDACi was hampered by pro-survival BCL2 family

members (Lindemann *et al*., 2007: Vrana, 1999). High MCL1 expression has been detected in about 70% of patients with gastric cancer and expression of MCL1 is an independent prognostic factor (Maeta *et al*., 2004). Reduction of MCL1 expression by an antisense oligonucleotide in NCI-N87 gastric cancer cells increased sensitivity towards docetaxel and cisplatin (Wacheck *et al.,* 2006). Recently, it was indicated that overexpression of the antiapoptotic protein MCL1 was sufficient to avoid apoptosis in c-MYC overexpressing non-small cell lung cancer (Allen *et al*., 2011). Hence, MCL1 might be important beyond gastric tumorigenesis and appears as a valid chemotherapeutic marker protein. In addition to MCL1, BCL_{XL} overexpression in gastric cancers is very common (Kondo *et al.,* 1998; Smith *et al*., 2006) and depletion of BCL_{XL} leads to an increased sensitivity of such cells towards extrinsic apoptosis (Kondo *et al*., 1996). Furthermore, *in vivo* study in mice indicated that coexpression of MCL1 and c-MYC could be a useful biomarker for identifying aggressive forms of non-small cell lung carcinoma and for predicting patient prognosis (Allen *et al*., 2011). Taken together, the observation that c-MYC controls expression of important prosurvival BCL2 family members might argue that c-MYC is an important factor in gastric cancer treatment.

The oncogene and basic helix-loop-helix leucine-zipper transcription factor c-MYC heterodimerizes with MAX. These bind to cis-acting elements, the so called E-boxes (characterized by CACGTG nucleotides) of cancer promoting genes (Eilers and Eisenman, 2008). Inhibition of c-MYC has recently been reported to be well tolerated *in vivo* and inhibition of c-MYC completely eradicated tumors in a murine Kras-dependent lung cancer model (Soucek *et al*., 2008). Therefore, several approaches to inhibit c-MYC are currently under development (Prochownik and Vogt, 2010). Overexpression of c-MYC has frequently been observed in gastric cancer (Calcagno *et al*., 2008) and is associated with therapeutic resistance of certain tumor entities (Leonetti *et al.,* 1999; Mizutani *et al*., 1994; Sklar and Prochownik, 1991). Furthermore, it has been indicated that c-MYC is highly deregulated in both intestinal and diffuse type of gastric cancer. Its deregulation is more common in precancerous and early gastric cancer tissues (Calcagno *et al*., 2008). A high affinity c-MYC binding site in the *MCL1* promoter has also been found in U937 histiocytoma cells (Fernandez *et al*., 2003). Consistent with the downregulation of MCL1 protein and mRNA after the knockdown of *c-MYC*, the binding of c-MYC to the *MCL1* promoter region in gastric cancer cell lines was detected, demonstrating direct transcriptional

regulation. In addition to c-MYC's direct transcriptional mode of action, this factor can regulate protein expression at the level of translation. The transcriptional factor c-MYC can control genes coding for translation initiation factors, such as eIF4E (Lin *et al*., 2008; Jones *et al*., 1996; Rosenwald *et al*., 1993). Dysregulated translational control can contribute to diverse human diseases, including cancer (Sonenberg and Hinnebusch, 2009). Translational initiation is regulated by the eIF4F complex, which is composed of the RNA helicase eIF4A, the scaffolding protein eIF4G and the cap-binding protein eIF4E, which is believed to be the rate limiting protein in the eIF4F complex (Fischer *et al*., 2009; Sonenberg and Hinnebusch, 2009). The translation initiation factor eIF4E has transforming characteristics *in vivo* and *in vitro* and was found to be overexpressed in various tumors, contributing to proliferation, survival, angiogenesis and metastasis of cancer cells (Fischer *et al*., 2009; Graff *et al*., 2008; Sonenberg and Hinnebusch, 2009). Also in gastric cancer patients, high expression of eIF4E was correlated with vascular invasion and a worse outcome of patients (Chen *et al*., 2004). This study demonstrates that c-MYC controls the transcription of *eIF4E* in gastric cancer cell lines by directly binding to its proximal high affinity E-box. Since the *eIF4E* knockdown results in a distinct downregulation of BCL_{XL}, these data illustrate that BCL_{XL} is regulated at the translational level in gastric cancer cell lines. This result is in line with observations from breast cancer models, in which the BCL_{XL} expression was reduced by knockdown of *eIF4E* (Soni *et al*., 2008). In contrast to the data obtained with HDACi in gastric cancer cells, there is evidence that c-MYC can promote the efficacy of diverse chemotherapeutics and γ-irradiation in other tumor entities (Larsson and Henriksson, 2010). While the molecular determinants that define the protherapeutic or therapeutic-resistance role of c-MYC are still equivocal, these data clearly argue for the need to determine the molecular actions of novel therapeutic strategies in pre-clinical settings, especially considering that even novel targeted therapies are used in combinations with conventional therapeutics. In this regard, it is demonstrated here that the anti-apoptotic BCL2 family members MCL1 and BCL_{XL} limit the biological effects HDACi exert against gastric cancer cells. Since MCL1 and BCL_{XL} are regulated by c-MYC in gastric cancer cells, c-MYC inhibition applied in combination with HDACi might be a rationally based therapeutic option for this type of cancer. Since c-MYC is included in a three gene predictor indicating poor prognosis for cisplatin/5-FU treated gastric cancer patients (Kim *et al*., 2011), c-MYC might limit the therapeutic response of gastric cancers beyond HDACi.

6. Conclusions

Despite temporal decline in gastric cancer incidence in several countries, it causes nearly 1 million deaths per year worldwide and is still a serious public health problem. Gastric cancer is usually diagnosed at advanced stages and the only available curative therapy requires surgical resection (Calcagno *et al*., 2008). The major problems that hamper improving the outcome of gastric cancer patients are:

1. Inavailabilty of biomarker molecules for detection of precancerous and cancerous lesions

2. Lack of efficient and minimal invasive therapy to cease the progress of early gastric cancer into adenocarcinomas.

To this end, this study contributes a considerable effort. Thus, the following conclusions are drawn from the current study:

1. Cathepsins and MMPs are promising biomarker molecules for early detection of gastric cancer. This is illustrated by their elevated expression in gastric cancer cell lines and tumor tissues but not in corresponding normal mucosa in murine gastric cancer model.

2. BCL_{XL} and MCL1 are important antiapoptotic proteins hampering the efficiency of HDACi in gastric cancer.

3. c-MYC regulates BCL_{XL} and MCL1 in gastric cancer, indicating that targeting c-MYC in combination with HDACi may improve the outcome of gastric cancer patients.

7. Bibliography

Akama, Y., Yasui, W., Yokozaki, H. *et al*. (1995). Frequent amplification of the cyclin E gene in human gastric carcinomas. *J Cancer Res 86*, 617-621.

Ali, S. H. and DeCaprio, J. A. (2001). Cellular transformation by SV40 large T antigen: interaction with host proteins. *Cancer biology 11*, 15-22.

Allen, T. D., Zhu, C. Q., Jones, K. D., *et al.* (2011). Interaction between *MYC* and *MCL1* in the Genesis and Outcome of Non-Small-Cell Lung Cancer. *Cancer Res 71*:2212-2221.

Amati, B., Dalton, S., Brooks, M. W. *et al*. (1992). Transcriptional activation by the human c-Myc oncoprotein in yeast requires interaction with Max. *Nature 359,* 423-426.

Blackwood, E. M., and Eisenman, R. N. (1991). Max: a helix–loop–helix zipper protein that forms a sequence-specific DNA-binding complex with Myc. *Science 251*, 1211-12127.

Bolden, E. J., Peart, J. M. Johnstone, W. R. (2006). Anticancer activities of histone deacetylase inhibitors. *Nature Rev Drug* discovery *5*, 769-784.

Bremer, C., Bredow, S., Mahmood, U. *et al*. (2001). Optical imaging of matrix metalloproteinase-2 activity in tumors:feasibility study in a mouse model. *Radiology. 221,* 523–529.

Busuttil, R. A., and Boussioutas, A. (2009). Intestinal metaplasia: A premalignant lesion involved in gastric carcinogenesis. *J Gastroenterol Hepatol 24***,** 193-201.

Carneiro, F., Oliveira, C., Suriano, G. *et al*. (2008). Molecular pathology of familial gastric cancer, with an emphasis on hereditary diffuse gastric cancer. *J Clin Pathol 61*, 25-30.

Catalano, V., Labianca, R., Beretta, G. D. *et al*. (2005). Gastric cancer. *Critical reviews in oncology/hematology 54*, 209-241.

Calcagno, D. Q., Leal, M. F., Assumpcao, P. P. *et al*. (2008). MYC and gastric adenocarcinoma carcinogenesis. *World J Gastroenterol 14*, 5962-5968.

Cavallo-Medved, D., Rudy, D., Blum, G. *et al*. (2009). Live-cell imaging demonstrates extracellular matrix degradation in association with active cathepsin B in

caveolae of endothelial cells during tube formation. *Experiment cell reserch 315*, 1234-1246.

Charlton, A., Blair, V., D. Shaw, D. *et al.* (2004). "Hereditary diffuse gastric cancer: predominance of multiple foci of signet ring cell carcinoma in distal stomach and transitional zone." *Gut 53*, 814-820.

Chen, C. N., Hsieh, F. J., Cheng, Y. M. *et al.* (2004). Expression of eukaryotic initiation factor 4E in gastric adenocarcinoma and its association with clinical outcome. *J Surg Oncol 86,* 22-27.

Chen, J. P., Lin, C., Xu, C.P. *et al*. (2001). Molecular therapy with recombinant antisense c-myc adenovirus for human gastric carcinoma cells *in vitro* and *in vivo. J Gastroenterol Hepatol 16,* 22-28.

Choi, J. H., Kwon, H. J., Yoon, B. I. *et al*. (2001). Expression profile of histone deacetylase 1 in gastric cancer tissues. *Jpn J Cancer Res 92*,1300-1304.

Clarke, P., Mann. J., Simpson, J. F. *et al.* (1998). Mice Transgenic for Human Carcinoembryonic Antigen as a Model for Immunotherapy. *Cancer Res 58*, 1469-1477.

Clyne, M., Dillon, P., Daly, S. *et al*. (2004). *Helicobacter pylori* interacts with the human single-domain trefoil protein TFF1. *Proc Natl Acad Sci U S A 101*, 7409-7414.

Compare, D., Rocco, A., and Nardone, G. *(*2010). Risk factors in gastric cancer. *Eur Rev Med Pharmacol Sci 14*, 302-308.

Correa, P., and Houghton, J. (2007). Carcinogenesis of *Helicobacter pylori. Gastroenterology 133*, 659- 672.

Correa, P., Haenszel, W., Cuello, C. *et al.* (1975). A model for gastric cancer epidemiology. *Lancet 2,* 58- 60.

Dang, C. V. (1999). c–Myc target genes involved in cell growth, apoptosis, and metabolism. *Mol Cell. Bio 19*, 1–11.

Dang, C. V., O'Donell, K. A., Zeller, K. I. *et al*. (2006). The c-Myc target gene network. *Semin Cancer Biol 16*, 253-264.

Deryugina, E. I., and Quigley, J. P. (2006). Matrix metalloproteinases and tumor

metastasis. *Cancer Metastasis Rev* 25, 9-34.

de Vries, A. C., Meijer, G. A., Looman, C. W. N. *et al.* (2007). Epidemiological trends of pre-malignant gastric lesions; a long-term nationwide study in the Netherlands. *Gut 56,* 1665-1670.

Eilers, M., and Eisenman, R. N. *(*2008). Myc's broad reach. *Genes Dev. 22*, 2755-2766.

El-Omar, E. M., Rabkin, C. S., Gammon, M. D. *et al*. (2003). Increased risk of noncardia gastric cancer associated with proinflammatory cytokine gene polymorphisms. *Gastroenterol 124,* 1193-1201.

Enns, R. (2010). Missed Cancers in the Upper Gastrointestinal Tract After Esophagogastroduodenoscopy. *Gastroenterol & Hepatol 6*, Issue 11

Eser, S., Messera, M., Eser, P. *et al*. (2011). *In vivo* diagnosis of murine pancreatic intraepithelial neoplasia and early-stage pancreatic cancer by molecular imaging. *PNAS Medical science*.

Fernandez, P.C., Frank, S. R., Wang, L. *et al*. (2003). Genomic targets of the human c-Myc protein. *Genes Dev 17*, 1115-1129.

Fischer, P. M. (2009). Cap in hand: targeting eIF4E. *Cell Cycle 8*, 2535-2541.

Fox, J. G. and Wang, T. C. (2007). Inflammation, atrophy, and gastric cancer. *J. Clin. Invest 117*, 60-69.

Franco, A. T., Israel, D. A., Washington, M. K. *et al*. (2005). Activation of β-catenin by carcinogenic *Helicobacter pylori*. *Proc Natl Acad Sci U S A 102,* 10646-10651.

Frew, A. J., Johnstone, R. W., Bolden, J. E. (2009). Enhancing the apoptotic and therapeutic effects of HDAC inhibitors. *Cancer Lett 280*, 125-133.

Gallinari, P., Di Marco, S., Jones, P. *et al*. (2007). HDACs, histone deacetylation and gene transcription: from molecular biology to cancer therapeutics. *Cell Res 17*, 195–211.

Glozak, M. A., and Seto, E. (2007). Histone deacetylases and cancer. *Oncogene 26,* 5420-5432.

Gocheva, V., and Joyce J.A. (2007). Cysteine Cathepsins and the Cutting Edge of Cancer Invasion. *Cell Cycle 6*, 60-64.

Gounaris, E., Tung, H. C., Restaino, C. *et al.* (2008). Live Imaging of Cysteine Cathepsin Activity Reveals Dynamics of Focal Inflammation, Angiogenesis, and Polyp Growth. *PLoS ONE 3*, Issue 8.

Graff, J. R., Konicek, B. W., Carter, J. H., Marcusson, E. G. (2008). Targeting the eukaryotic translation initiation factor 4E for cancer therapy. *Cancer Res 68,* 631-634.

Grandori, C., Cowley, S. MJames, L. P. *et al*. (2000). The MYC/MAX/MAD net work and the transcriptional control of cell behavior. *Annu. Rev. Cell Dev. Biol 16*, 653-699.

Gravalos, C., and Jimeno, A. (2008). HER2 in gastric cancer: a new prognostic factor and a novel therapeutic target. *Ann Oncol 19*, 1523-1529.

Guilford, P., Hopkins, J., Harraway, J. *et al*. (1998). E-cadherin germline mutations in familial gastric cancer. *Nature 392*, 402-405.

Guo, B. X., Jing, C., Li, L. *et al*. (2011). Down-regulation of miR-622 in gastric cancer promotes cellular invasion and tumor metastasis by targeting ING1 gene. *World J Gastroenterol 14*, 1895-1902.

Haglund, U. H., Wallner, B. (2004). Current Management of Gastric Cancer. The Society for Surgery of the Alimentary Tract. *Published by Elsevier Inc*, 905-912.

Han. S., Kim, H. Y., Park, K., *et al.* (1999). c-Myc expression is related with cell proliferation and associated with poor clinical outcome in human gastric cancer. *J Korean Med Sci 14*, 526-530.

Hance, K.W., Zeytin, H.E., Greiner, J.W. (2005). Mouse models expressing human carcinoembryonic antigen (CEA) as a transgene: evaluation of CEA-based cancer vaccines. *Mutat Res 576* (1-2), 132.

Hartgrink, H. H., Jansen, E. P. M., van Grieken, N. C. T. *et al*. (2009). Seminar on: Gastric cancer. *Lancet 374*, 477-490.

Hattori, Y., Odagiri, H., Nakatani, H. *et al.* (1990). K-*sam*, an amplified gene in stomach cancer, is a member of the heparin-binding growth factor receptor genes. *Proc Natl Acad Sci USA 87*, 5983-5987.

Herszényi, L., Farinati, L., Cardin, R. *et al*. (2008). Tumor marker utility and prognostic relevance of cathepsin B, cathepsin L, urokinase-type plasminogen

activator, plasminogen activator inhibitor type-1, CEA and CA 19-9 in colorectal cancer. *BMC Cancer 8*:194.

Hess-Stumpp, H., Bracker, T. U., Henderson, D. *et al*. (2007). MS-275, a potent orally available inhibitor of histone deacetylases-the development of an anticancer agent. *Int J Biochem Cell Biol 39*, 1388-1405.

Hu, Z., Ajani, J. A., Wie, Q. (2007). Molecular Epidemiology of Gastric Cancer: Current Status and Future Prospects. *Gastrointest Cancer Res 1*, 12-19.

Jemal, A., Siegel, R., Ward, E., *et al*. (2007). Cancer statistics. *CA Cancer J Clin 57*, 43-46.

Johnson, S. M., Evers, B. M. (2008). Translational research in gastric malignancy. *Surg Oncol Clin N Am 17*, 323-340.

Jones, R. M., Branda, J., Johnston, K. A. et al. (1996). An essential E box in the promoter of the gene encoding the mRNA cap-binding protein (eukaryotic initiation factor 4E) is a target for activation by c-myc. *Mol Cell Biol 16*, 4754-4564.

Joossens, J. V., Hill, M. J., Elliott, P. *et al*. (1996). Dietry salt, nitrate and stomach cancer mortality in 24 countries. *Int J Epidemiol 25*, 494.

Keppler, D., Sameni, M., Moin, K. *et al.* (1996). Tumor progression and angiogenesis: cathepsin B & Co. Biochem. *Cell Biol 74,*799–810.

Khanna, A., Bockelman, C., Hemmes, A. *et al.* (2009). MYC-dependent regulation and prognostic role of CIP2A in gastric cancer*. J Natl Cancer Inst 101*, 793-805.

Kim, H. K., Choi, I. J., Kim, C. G. *et al*. (2011). Three-gene predictor of clinical outcome for gastric cancer patients treated with chemotherapy. *Pharmacogenomics J* [Epub ahead of print].

Kondo, S., Shinomura, Y., Kanayama, S. *et al.* (1996). Over-expression of bcl-$_{xL}$ gene in human gastric adenomas and carcinomas. *Int J Cancer 68,* 727-730.

Kondo. S., Shinomura, Y., Kanayama, S. *et al*. (1998). Modulation of apoptosis by endogenous Bcl_{XL} expression in MKN-45 human gastric cancer cells. *Oncogene 17*, 2585-2591.

Kono, S., and Hirohata, T. (1996). Nutrition and stomach cancer. *Cancer causes control 7*, 41.

Koopman, G., Reutelingsperger, C. P., Kuijten, G. A. *et al*. (1994). Annexin V for flow cytometric detection of phosphatidylserine expression on B cells undergoing apoptosis. *Blood 84*, 1415-1420.

Kuester, D. Lippert, H. Roessner, A. *et al*. (2008). The cathepsin family and their role in colorectal cancer. *Pathology–Research and Practice 204*, 491–500.

Kuniyasu, H., Yasui, W., Kitadai, Y. *et al*. (1992). Frequent amplification of the c-*met* gene in scirrhous type stomach cancer. *Biochem Biophys Res Commun 189*, 227-232.

Lan, J., Xiong, Y. Y., Lin, Y. X. *et al.* (2003). *Helicobacter pylori* infection generated gastric cancer through p53-Rb tumor-suppressor system mutation and telomerase reactivation. *World J Gastroenterol 9,* 54-58.

Lambert, R. (2002). Diagnosis of esophagogastric tumors. *Eondoscopy 34*,129-138.

Larsson, L. G., Henriksson, M. A. (2010). The Yin and Yang functions of the Myc oncoprotein in cancer development and as targets for therapy. *Exp Cell Res 316,* 1429-1437.

Latt, S. A., Stetten, G., Juergens, L. A. *et al.* (1975). Recent developments in the detection of deoxyribonucleic acid synthesis by 33258 Hoechst fluorescence. *Journal of the Histochemistry Society 23,* 493-505.

Lefebvre, O., Chenard, M. P., Masson, R. *et al.* (1996). Gastric mucosa abnormalities and tumorigenesis in mice lacking the pS2 trefoil protein. *Science 274*, 259-262.

Leodolter, A., Kulig, M., Brasch, H. *et al.* (2006). A meta-analysis comparing eradication, healing and relapse rates in patients with Helicobacter pylori-associated gastric or duodenal ulcer. *Aliment Pharm Ther 15,* 1949-1958.

Leonetti, C., Biroccio, A., Candiloro, A. *et al.* (1999). Increase of cisplatin sensitivity by c-myc antisense oligodeoxynucleotides in a humanmetastatic melanoma inherently resistant to cisplatin. *Clin Cancer Res 5*, 2588-2595.

Lindemann, R. K., Newbold, A., Whitecross, K. F. *et al*. (2007). Analysis of the apoptotic and therapeutic activities of histone deacetylase inhibitors by using a mouse model of B cell lymphoma. *Proc Natl Acad Sci U S A 104*, 8071-8076.

Lin, C. J., Cencic, R., Mills, J.R. *et al.* (2008). c-Myc and eIF4F are components of a feedforward loop that links transcription and translation. *Cancer Res 68*, 5326-5334.

Lochhead, P., and El-Omar, M.E. (2008). Review on: Gastric cancer. *British Medical Bulletin 85*, 87-100.

Lynch, H. T., Grady, W., Suriano, G., Huntsman, D. (2005). Gastric cancer: new genetic developments. *J Surg Oncol 90,* 114-133.

MacDonald, J. S., Smalley, S. R., Benedetti, J. *et al.* (2003). Chemoradiotherapy after surgery compared with surgery alone for adenocarcinoma of the stomach or gastroesophageal junction. *N Engl J Med 345*, 725-730.

Machado, J. C., Figueiredo, C., Canedo, P. *et al*. (2003). A proinflammatory genetic profile increases the risk for chronic atrophic gastritis and gastric carcinoma. *Gastroenterology 125*, 364-371.

Machado, J. C., Pharoah, P., Sousa, S. *et al.* (2001). Interleukin 1B and interleukin 1RN polymorphisms are associated with increased risk of gastric carcinoma. *Gastroenterology 121*, 823-829.

Machado, J. C., Soares, P., Carneiro, F. *et al.* (1999). E-cadherin gene mutations provide a genetic basis for the phenotypic divergence of mixed gastric carcinomas. *Lab Invest 79*, 459-465.

Maeta, Y., Tsujitani, S., Matsumoto, S*. et al.* (2004). Expression of Mcl-1 and p53 proteins predicts the survival of patients with T3 gastric carcinoma. *Gastric Cancer 7*, 78-84.

Mahmood, U. and Weissleder, R. (2003). Near-Infrared Optical Imaging of Proteases in Cancer. *Mol Cancer Ther 2,* 489-496.

Marks, P. A., Richon, V. M., Miller, T. *et al.* (2003). Histone deacetylase inhibitors. *Adv Cancer Res 91***,** 137-168.

Marks, P. A., Rifkind, R. A., Richon, V. M. *et al.* (2001). Histone deacetylases and cancer: causes and therapies. *Nat Rev Cancer 1*, 194-202.

Marks, P. A., Xu, W. S. (2010). Histone deacetylase inhibitors: potential in cancer therapy*. J Cell Biochem 107,* 600-608.

Martin, R. C., Jaques, D. P., Brennan, M., F. Karpeh, M. (2002). Extended local resection for advanced gastric cancer: increased survival versus increased morbidity. *Ann sug 236,* 159-*165*.

McMahon, S. B. (2010). Emerging Concepts in the Analysis of Transcriptional Targets of the MYC Oncoprotein: Are the Targets Targetable? *Genes & Cancer 1*, 560-567.

Meyer, N., and Penn, L. Z. (2008). Reflecting on 25 years with MYC. *Nature reviews 8*, 976-990.

Milne, A. N., Sitarz, R., Carvalho, R. *et al.* (2007). Early onset gastric cancer: on the road to unraveling gastric carcinogenesis. *Curr Mol Med 7,* 15-28.

Minucci, S., and Pelicci, P. G. (2006). Histone deacetylase inhibitors and the promise of epigenetic (and more) treatments for cancer. *Nat Rev Cancer 6*, 38-51.

Mizutani, Y., Fukumoto, M., Bonavida, B. *et al.* (1994). Enhancement of sensitivity of urinary bladder tumor cells to cisplatin by c-myc antisense oligonucleotide. *Cancer 74,* 2546-2554.

Mohamed, M. M., Sloane, B. F. (2006). Cysteine cathepsins: Multifunctional enzymes in cancer. *Nat Rev Cancer* 6, 764-75.

Mosmann, T. (1983). Rapid colorimetric assay for cellular growth and survival: application to proliferation and cytotoxicity assays. *J Immunol Methods 65,* 55-63.

Müller, S., and Krämer, O. H. (2010). Inhibitors of HDACs-effective drugs against cancer? *Curr Cancer Drug Targets 10*, 210-28.

Münster, M. N., Thurn, K. T., Thomas, S. *et al*. (2011). A phase II study of the histone deacetylase inhibitor vorinostat combined with tamoxifen for the treatment of patients with hormone therapy-resistant breast cancer. *British Journal of Cancer 104*, 1828-1835

Murphy, G. (2008). The ADAMs: signalling scissors in the tumour microenvironment. Nat. Rev. Cancer *8,* 929-941.

Murphy, G., and Nagase, H. (2008). Progress in matrix metalloproteinase research. Mol. Aspects Med. *29,* 290-308.

Mutze, K., Langer, R., Becker, K. *et al*. (2010). Histone deacetylase (HDAC) 1 and 2 expression and chemotherapy in gastric cancer. *Anals of surgical oncology 17*, 3336-3343.

Nakatsuru, S., Yanagisawa, A., Ichii, S. *et al*. (1992). Somatic mutation of the APC gene in gastric cancer: frequent mutations in very well differentiated adenocarcinoma and signet-ring cell carcinoma. *Hum Mol Genet 1*, 559- 563.

Nilsson, J. A., and Cleveland, J. L. (2003). Myc pathways provoking cell suicide and cancer. *Oncogene 22,* 9007–9021.

Nöckel, J., den Engel, N. K., Winter, H. *et al*. (2006). Characterization of gastric adenocarcinoma cell lines established from CEA424/SV40 T antigen-transgenic mice without a human CEA transgen. *BMC Cancer 6*: 57

Parkin, D. M., Pisani, P., and Ferlay, J. (1999). Global cancer statistics. *CA Cancer J Clin 49,* 33-64.

Patel, J. H., Loboda, A. P., Showe, M. K. *et al.* (2004). Analysis of genomic targets reveals complex functions of MYC. *Nat Rev Cancer 4*, 562-568.

Peek, R. M., Blaser, M. J. (2002). Helicobacter pylori and gastrointestinal tract adenocarcinomas. *Nat Rev Cancer 2,* 28-37.

Pelengaris, S., Khan, M., Evan, G. (2002). c-MYC: more than just a matter of life and death. *Nat Rev Cancer 2*, 764-776.

Peleteiro, B., Lopes, C., Figueiredo, C. *et al.* (2011). Salt intake and gastric cancer risk according to *Helicobacter pylori* infection, smoking, tumor site and histological type. *Br J Cancer 104*,198.

Prochownik, E. V., and Vogt, P. K. (2010). Therapeutic Targeting of Myc. *Genes Cancer 1,* 650-659.

Rosenwald, I. B., Rhoads, D. B., Callanan, L.D. et al. (1993). Increased expression of eukaryotic translation initiation factors eIF4E and eIF2-alpha in response to growth induction by c-myc. *Proc Natl Acad Sci U S A 90*, 6175-6178.

Rugge, M., Cassaro, M., Di Mario, F. *et al*. (2003). The long term outcome of gastric non-invasive neoplasia: for the Interdisciplinary Group on Gastric Epithelial Dysplasia (IGGED). *Gut 52*, 1111-1116.

Shang, J., and Pena, A. S. (2005). Multidisciplinary approach to understand the

pathogenesis of gastric cancer. *World J Gastroenterol 11*, 4131-4139.

Shikata, K., Kiyohara, Y., kubo, M. *et al.* (2006). A prospective study of dietry salt intake and gastric cancer incidence in a defined Japanese population. *Int J cancer 119*, 196.

Schmidt, E. V. (2004). The role of c-myc in regulation of translation initiation. *Oncogene 23,* 3217-3221.

Sklar, M. D., Prochownik, E.V. (1991). Modulation of cis-platinum resistance in Friend erythroleukemia cells by c-myc. *Cancer Res 51*, 2118-2123.

Skoudy, A., Hernández-Muñoz, I., Navarro, P. (2011). Pancreatic Ductal Adenocarcinoma and Transcription Factors: Role of c-Myc. *J Gastrointest Canc 42*, 76-84.

Smith, M. G., Hold, G. L., Tahara, E., and El-Omar, E. M. (2006). Cellular and molecular aspects of gastric cancer. *World J Gastroenterol 12*, 2979-2990.

Smith, L., Berrieman, H. K., O'Kane, S. L. *et al*. (2006). Immunohistochemical detection of apoptotic markers in gastric cancer. *Oncol Res 15*, 441-444.

Sonenberg, N., and Hinnebusch, A. G (2009). Regulation of translation initiation in eukaryotes: mechanisms and biological targets. *Cell 136,* 731-745.

Soni, A., Akcakanat, A., Singh, G. *et al.* (2008). *eIF4E* knockdown decreases breast cancer cell growth without activating Akt signaling. *Mol Cancer Ther 7,* 1782-1788.

Soucek, L., Whitfield, J., Martins, C. P. *et al*. (2008). Modelling Myc inhibition as a cancer therapy. *Nature 455,* 679-683.

Spange, S., Wagner, T., Heinzel, T. *et al*. (2009). Acetylation of non-histone proteins modulates cellular signalling at multiple levels*. Int J Biochem Cell Biol 41,* 185-198.

Tabernero, J., Macarulla, T., Ramos, F. J. *et al*. (2005). Novel targeted therapies in the treatment of gastric and esophageal cancer. *Ann Oncol 16*, 1740-1748.

Tahara, E. (2004). Genetic pathways of two types of gastric cancer. *IARC Sci Publ* 327- 349.

Telford, J. J. and Enns, R. A. (2010). Endoscopic Missed Rates of Upper Gastrointestinal Cancers: Parallels with Colonoscopy. *Am J Gastroenterol 105,* 1298–1300

Thompson, J. A., Eades-Perner, A. M., Ditter, M. *et al*. (1997). Expression of transgenic carcinoembryonic antigen (CEA) in tumor-prone mice: an animal model for CEA-directed tumor immunotherapy. *Int J Cancer 72,* 197-202.

Thompson, J., Epting, T., Schwarzkopf, G. *et al.* (2000). A transgenic mouse line that develops early-onset invasive gastric carcinoma provides a model for carcinoembryonic antigen-targeted tumor therapy. *Int J Cancer 86,* 863-869.

Tsugane, S., Sasazuki, S. (2007). Diet and the risk of gastric cancer: review of epidemiological evidence. Gastric cancer *10*, 75.

Vrana, J. A. Decker, R. H. Johnson, C. R. *et al*. (1999). Induction of apoptosis in U937 human leukemia cells by suberoylanilide hydroxamic acid (SAHA) proceeds through pathways that are regulated by Bcl-2/Bcl-XL, c-Jun, and $p21^{CIP1}$, but independent of p53. *Oncogene 18*, 7016-7025.

von Burstin, J., Eser, S., Seidler, B., *et al*. (2008). Highly sensitive detection of early-stage pancreatic cancer by multimodal near-infrared molecular imaging in living mice. *Int J Cancer 123*, 2138-2147.

Wacheck, V., Cejka, D., Sieghart, W. *et al.* (2006). Mcl-1 is a relevant molecular target for antisense oligonucleotide strategies in gastric cancer cells. *Cancer Biol Ther 5*, 1348-1354.

Wagner, A. D., Unverzagt, S., Grothe, W. *et al*. (2005). Chemotherapy for advanced gastric cancer. *Cochrane Database Syst Rev*: CD004064.

Walkinshaw, D. R., and Yang, X. J. (2008). Histone deacetylase inhibitors as novel anticancer therapeutics. *CURRENT ONCOLOGY 15*, 237-243.

Weichert, W., Roske, A., Gekeler, V. *et al*. (2008). Association of patterns of class I histone deacetylase expression with patient prognosis in gastric cancer: a retrospective analysis. *Lancet Oncol 9,* 139-48.

Weissleder, R. (2006). Molecular imaging in cancer. *Science 312,* 1168-1171.

Weissleder, R., and Mahmood, U. (2001). Molecular imaging, Radiology, *219:* 316–333

Weissleder, R. and Ntziachristos, V. (2003). Shedding light onto live molecular targets. NATURE MEDICINE 9, 1.

Wiedemann, T., Loell, E., Mueller, S. et al. (2009). Helicobacter pylori cag-Pathogenicity Island-Dependent Early Immunological Response Triggers Later Precancerous Gastric Changes in Mongolian Gerbils. *PLoS ONE 4*, issue 3.

Wirth. M., Fritsche, P., Stojanovic, N. *et al.* (2011). Simple and cost-effective method to transfect small interfering RNAs into pancreatic cancer cell lines using polyethylenimine. *Pancreas 40*, 144-150.

World Health Organization (WHO) (2003). Diet, nutrition, and the prevention of chronic diseases. *WHO technical report series 916.* Geneva.

Xu, W. S., Parmigiani, R. B., and Marks, P. A. (2007). Histone deacetylase inhibitors: molecular mechanisms of action. *Oncogene 26*, 5541-5552.

Yang, X. J., and Seto, E. (2008). The Rpd3/Hda1 family of lysine deacetylases: from bacteria and yeast to mice and men. *Nat Rev Mol Cell Biol 9,* 206-218.

Yin, X., Giap, C., Lazo, J.S. et al. (2003). Low molecular weight inhibitors of Myc-Max interaction and function. *Oncogene 22,* 6151-6159.

Yokozaki, H., Ito, R., Nakayama, H. *et al.* (1994). Expression of CD44 abnormal transcripts in human gastric carcinomas. *Cancer Lett 83*, 229-234.

Yokozaki, H., Kuniyasu, H., Kitadai, Y. *et al*. (1992). p53 point mutations in primary human gastric carcinomas. *J Cancer Res Clin Oncol 119*, 67-70.

Zhang, L., Hou, Y., Ashktorab, H. *et al*. (2010). The impact of C-MYC gene expression on gastric cancer cell. *Mol Cell Biochem 344*, 125-135.

8. Lebenslauf

i. Persönliche Daten

Name	Labisso, Wajana Lako
Geburtsdatum	14.06.1979
Geburtsort	Wolayta Soddo (Southern Ethiopia)
Geschlecht	Männlich
Familienstand	Verheiratet
Religion	Romanische Katholisch
Staatsbürgerschaft	Äthiopien
Anschrift	e-mail:wajaliya@googlemail.com Tel. +4917694505117

ii. AUSBILDUNG

Jahr	specialization
1988-1996	Grundschule , Shanto Grudnschule,Ethiopia
1996-1999	Gym. St. Joseph Gym. Nazareth, Ethiopia
1999-2003	Bachelor in Biologie, Universität Bahir Dar, Ethiopia
2005-2007	M.Sc in Biologie (Applied microbiologie), Universität Addis Ababa, Ethiopia
2008-2012	Promotion an der TU München

iii. Sprachkennetnisse

Englisch	Sehr gut
German	Gut
Amharic	Sehr gut
Wolayta	Muttersprach
Orromiffa	Gut

iv. Publikation und Thseis

1) “MYC directs transcription of *MCL1* and *eIF4E* genes to control sensitivity of gastric cancer cells towards HDAC inhibitors”, accepted for publication in cell cycle.
2) Isolation and characterization of cyanide degrading bacteria from Ethiopian alkaline soda lakes (Lake Chitu). MSc. thesis.
3) Early Detection and Treatment evaluation of Gastric Cancer. PhD thesis.

9. Acknowledgements

First of all, my genuine gratitude goes to Prof. Dr. Roland Schmid for allowing me to use all the facilities in “II Medizinische Klinik des Klinikums rechts der Isar” for my PhD work. I would like to thank Prof. Dr. Angelika Schnieke, the external supervisor of my PhD study, for her remarkable support throughout my study.

My heartfelt gratitude goes to my PhD supervisor, PD. Dr. Dieter Saur, for providing me the opportunity to work in his laboratory. Not only the scientific and experienced support but also his friendly discussions and readiness to help when needed brought my study a fruitful end.
Of course, I am very grateful to PD. Dr. Günter Schneider for his continuous help in shaping this project. I really appreciate his critical suggestions and dynamic scientific approaches to solve problems. His friendly discussions and guidance made this project possible.

It is my pleasure to take this opportunity to thank **KAAD** (Katholischer Akademischer Ausländer-Dienst) for the scholarship grant for my PhD study at Technical University of Munich. Particularly, the Africa department representatives: Simone Saure and Dr. Marko Kuhn deserve greatest thanks for their fantastic sense of humor, friendly approach and fascinate concern.

My special thanks goes to all colleagues in the working group of Dr. Saur and Dr. Schneider for the nice working atmosphere and good collaboration, especially for helpful assistance of all the lab experts and their informal tutoring in the lab. I would like to convey my gratitude to everybody who supported me with comments, discussion, editing or helpful ideas to realize this work. In this regard, special thanks go to Matthias Wirth, Mariel Paul, Barbara Seidler and Dereje Woldemedhin. I am also grateful to Dr. Raquel Mejías-Luque for her kind gifts of cell lines.

My wife, Tsion Orlando, and my daughter, Liya Wajana, deserve my heartfelt gratitude for their love and care. Dear Tsion, I could understand the pain of loneliness but it was for good mission and now we are on the verge of harvesting the fruit of our patience.

Above all, I am really adoringly thankful to almighty God for His being with me throughout my life, particularly during my PhD study!!